PDL-1+ Neutrophils mediate susceptibility during endotoxemia in Metabolic Dysfunction–Associated Steatotic Liver Disease

Cleyson da Cruz Oliveira Barros[1,2*], Alexandre Kanashiro[1,2*], Gabriel Victor Lucena da Silva[1,2], Paulo Sérgio de Almeida Augusto[1,2] , Guilherme Cesar Martelossi Cebinelli[1,2],; Luiz Osório Leiria[1,2], Thiago Mattar Cunha[1,2], José Carlos Alves Filho[1,2], and Fernando Queiroz Cunha[1,2]

[1]Center for Research in Inflammatory Diseases (CRID), Ribeirão Preto Medical School, University of São Paulo, Av. Bandeirantes; Rua das Paineiras, Casa 3, Ribeirão Preto, São Paulo, 14049-900, Brazil.

[2]Department of Pharmacology, Ribeirão Preto Medical School, University of São Paulo, Ribeirão Preto, São Paulo, Brazil.

*These authors contributed equally to this work

e-mail: fqdcunha@fmrp.usp.br

Abstract

Metabolic Dysfunction–Associated Steatotic Liver Disease (MAFLD) is a pathological condition affecting many individuals worldwide. Patients with MAFLD are more susceptible to systemic inflammation, including endotoxemia, which accelerates the progressive liver damage. However, the immunological mechanisms that trigger the hyper-inflammatory responses in individuals with MAFLD remain unknown. In the present study, we reported that short-term HFCD (Choline Deficient High Fat Diet)-fed mice, which did not show significant signs of hepatic damage and inflammation in the first two weeks, are more susceptible to a non-severe sepsis-like systemic inflammation induced by LPS challenge. Mechanistically, endotoxemic mice show an excessive accumulation of NK-producing IFN-γ cells in liver tissue, which trigger the recruitment and polarization of a distinct subset of neutrophils, characterized by high expression of PD-L1 and massive release of TNF-α. Remarkably, genetic inhibition of IFN-γ or pharmacological blockade of PD-L1 effectively modulated the excessive recruitment of these neutrophils to the liver and TNF-α production, thereby preventing hepatic damage and reducing the severity of host mortality. Thus, these results support the design of novel effective strategies to control hyperinflammatory responses in septic HFCD patients and consequently improve their survival.

Key Words: neutrophil; MAFLD; endotoxemia; PDL-1.

1. INTRODUCTION

Metabolic Dysfunction–Associated Steatotic Liver Disease (MAFLD), previously described as non-alcoholic fatty liver disease (NAFLD), is a metabolic liver dysfunction defined as an abnormal accumulation of fat in the liver without secondary triggers such as alcohol consumption. MAFLD has become a common chronic liver disease in the world population and has a high prevalence varying from simple steatosis to non-alcoholic steatohepatitis, fibrosis, cirrhosis, and hepatocellular carcinoma (1–3). Despite its high prevalence and increasing cause of liver-related mortality worldwide, MAFLD is still underestimated, and there are no approved pharmacological or preventive strategies for these medical conditions (4, 5).

The MAFLD is a highly complex condition that involves a “multi-hit” process, in which different stimuli act together to promote fat accumulation and progressive liver damage (6). Although the pathogenesis of MAFLD is multifactorial, inflammation has now been considered a key factor in the progression of advanced hepatic conditions (7–9). In the presence of obesity and lipotoxicity, the immune system is activated in the liver, with a corresponding degree of inflammation triggered by the “wound healing response”. Since these inflammatory signs persist for a long period, monocytes and neutrophils, as well as T CD4, T CD8, and natural killer (NK), can be recruited to the liver, releasing a massive secretion of pro-inflammatory cytokines, including interferon-gamma (IFN-γ) and tumor necrosis factor (TNF-α) (7, 10). Likewise, in chronic diseases, these cytokines are also present in systemic and uncontrolled inflammatory processes, such as sepsis (11). Sepsis is a syndrome characterized by a life-threatening dysfunction due to complex interactions between pathogens and the host recruitment of immune cells, resulting in a systemic hyper-inflammatory state followed by extensive vital organ damage, including in the liver (12, 13). Sepsis has also been considered the leading cause of death in intensive care units. In endotoxemia, a well-established sepsis model, this massive production of cytokines provokes uncontrolled recruitment of innate immune cells, mainly monocytes and neutrophils, to vital organs, including the liver, where they induce extensive and lethal damage (11, 14, 15). The majority of data regarding endotoxemia pathogenesis has focused only on the interaction between the infection and the host immune system, and only a few studies have addressed one or more clinical conditions that are considered risk factors leading to endotoxemia aggravation, such as senescence and previous immunosuppressive comorbidities (16–18). Thus, understanding how these

clinical conditions can modify the host immune response and consequently affect the outcome of sepsis is crucial to detecting the risks and designing novel preventive and therapeutic approaches to control exacerbated inflammatory responses. Recently, some population studies, including large-scale data from cohorts with biopsy-confirmed individuals, have evidenced a higher incidence of severe infections in MAFLD patients~~,~~ suggesting that previous hepatic conditions can modify the host immune response, leading to sepsis aggravation (19). However, although a relationship between elevated risk of sepsis in MAFLD patients exists, the underlying immunological mechanisms involved in the progression and exacerbation of systemic and/or local (hepatic) inflammation in these individuals have not been identified yet.

To understand the impact of MAFLD on liver damage during endotoxemia, we used a known murine model of MAFLD and later challenged these animals with a moderate dose of lipopolysaccharide (LPS). We demonstrated that endotoxemia exacerbated the hepatic inflammatory response and mortality in Choline Deficient High Fat Diet (HFCD)-fed mice. The LPS-activated hepatic NK cells secrete IFN-γ, which induces massive recruitment and polarization of a specific subpopulation of PD-L1-expressing neutrophils. This subpopulation of neutrophils releases a high concentration of TNF-α, which mediates the liver lesion and increases the mortality of the animals. In fact, biological treatments promoting PD-L1 neutralization, or neutrophil depletion, reduced the TNF-α concentration, the liver inflammatory response and organ pathology, and increased the survival in endotoxemic HFCD fed mice. Similar results were observed with the use of genetic knockout TNF-α receptor mice. Thus, our findings describe the potential mechanism involved in the exacerbation of neutrophil functions in MAFLD mice and suggest a viable approach to the development of individual interventions capable of mitigating the hyperinflammation observed in these pathological conditions.

2. RESULTS

MAFLD mice are more susceptible to LPS-induced systemic inflammation.

To study MAFLD as a pre-condition associated with increasing risk of exacerbation of inflammation induced by endotoxemia, we employed a murine model of MAFLD in which the mice were fed for two weeks with a choline-deficient high-fat HFCD diet, a well-known liver disease model (Fig. 1A). Therefore, we adopted a two-week HFCD feeding period, during which no changes in lymphocyte numbers were observed, as longer exposure to the choline-deficient HFCD is known to reduce lymphocyte numbers in mice (20). Mice fed HFCD showed no increase in liver weight and collagen deposition as evidenced by picrosirius staining (Fig. S1A and Fig. S1C). The HFCD mice challenged with LPS (10 mg/kg; intraperitoneally) triggered an elevated susceptibility with an index of mortality of 100% 24 h after the challenge (Fig. 1B). In our experimental condition, this dose of LPS provoked moderate (below 40%, 4 days after LPS challenge) mortality in chow-fed mice (control group) (Fig. 1B). Compared with the control group, the HFCD animals challenged with LPS showed elevated liver damage, evidenced by an increase in plasma alanine aminotransferase (ALT) levels (a known marker of liver injury) and histopathological alteration, characterized by leukocyte infiltration and edema (Fig 1C,1E). Compared with control mice treated with PBS, the HFCD animals also treated with PBS did not show significant signs of hepatic damage and local inflammatory response, evidenced by the absence of leukocyte infiltration (Fig. 1C and 1E). Animals subjected to the HFCD diet showed reduced blood glucose levels with or without LPS challenge (Fig. S1B). Remarkably, compared to the Chow group, HFCD mice exposed to LPS did not show greater changes in other organs commonly affected by endotoxemia, such as the kidneys (Figure 1D), indicating that a pathological inflammatory condition is increased mainly in liver tissue compared to other organs. To assess how MAFLD modulates the immune response in the hepatic microenvironment of human patients, we reanalyzed previously published bulk RNA-seq data from patients with MAFLD to identify potential targets related to the inflammatory process (21). First, we performed analyses of genes differentially expressed in leukocyte samples from patients with MAFLD and healthy controls. We observed that 5240 genes are upregulated, such as *EIF4H*, *TMEM*, *MOB1A*, *SERBP1*, *TM9SF1*, *HINT3*, *ARF3*, *CHTF8*, and *PDIA6*, while 5806 genes, as *FOSB*, *KAT2A*, *SNRNP70*, *CCNL2*, *AMY2B*, *EXD3*, and *EBNA1BP2, are*

141 downregulated. Interestingly, we found that the *CD274* gene (encoding PD-L1) and
142 the *IFNGR2* gene, corresponding to the IFN-γ receptor, are among the upregulated
143 genes (Fig. 2A). Furthermore, after conducting an additional enrichment analysis of
144 the 5240 upregulated genes using Gene Ontology (GO), we detected an increase in
145 several pathways associated with inflammatory processes, such as phagocytosis,
146 leukocyte migration, immune response to bacterial components, and signaling
147 pathways involving IL-1β, TNF-α, and IFN-γ (Fig. 2B).

148 Because IFN-γ and TNF-α signaling pathways are upregulated in MAFLD
149 patients, we reanalyzed previously published single-cell RNA-seq data from liver
150 samples from mice fed with a 60% high-fat diet, another known MAFLD model (22).
151 We noticed an increase in immune cells in the hepatic tissue, such as monocytes,
152 neutrophils, dendritic cells, T cells, and NK cells (Fig. 2C and 2D). Interestingly, we
153 observed a specific upregulation of CD274 and TNF-α genes in monocytes and
154 neutrophils, while T cells and NK cells showed increased IFN-γ expression (Fig. 2E),
155 suggesting that the cytokines produced by these specific cells may be involved in the
156 hyperinflammation observed during MAFLD.

157 Next, based on the results of increased IFN-γ and TNF-α signaling in bulk
158 RNAseq and single-cell RNA sequencing analyses in hepatic samples of MAFLD
159 patients and animals, we investigated the role of these cytokines in the susceptibility
160 of endotoxemic MAFLD mice. Initially, we observed an exacerbated hepatic production
161 of both cytokines induced by endotoxin challenge in the HFCD-fed group compared to
162 the control mice treated with PBS or LPS (Fig. 3A and 3B). Furthermore, we also
163 observed that IFN-$\gamma^{-/-}$ and TNFR1R2$\alpha^{-/-}$ mice with MAFLD challenged with LPS did not
164 show an increase in the enzyme ALT, a liver lesion marker (Fig. 3C and 3D). In
165 addition, endotoxemic MAFLD TNFR1R2$^{-/-}$ and IFN-$\gamma^{-/-}$ mice exhibited reduced
166 leukocyte infiltration in the liver tissue and improved survival (Fig. 3E, 3F, and 3G),
167 respectively, as compared to endotoxemic WT mice. Furthermore, splenocytes from
168 HFCD-fed IFN-deficient animals exhibited increased IL-6 and TNF-α production upon
169 *in vitro* LPS stimulation, indicating a response pattern similar to that of control animals
170 (Fig 2SA and Fig. 2SB). Together, our data demonstrate that MAFLD predisposes to
171 the exacerbation of cytokine production, such as IFN-γ and TNF-α, which mediate an
172 elevated index of mortality in endotoxemic mice.
173

174 **MAFLD induces the recruitment of NK cells that are sources of IFN-γ**
175 **production in endotoxemia**

176 During the inflammatory process, it is already established that CD4 and CD8 T
177 cells are important sources of IFN-γ(23). Herein, we observed a selective increase in
178 IFN-γ production by CD8, but not CD4, T cells during endotoxemia (Fig. 4A, Fig. 4B,
179 Fig. S3A, Fig. S3B), respectively. In light of this, we next investigated the involvement
180 of lymphoid cells in the high susceptibility of endotoxemic mice with MAFLD. To
181 address this question, Rag1^{-}/$^{-}$ mice, which lack T and B cells, were subjected to the
182 MAFLD protocol and then challenged with LPS, after which survival was assessed.
183 Interestingly, *Rag1*-deficient animals under the HFCD remained susceptible to the
184 LPS challenge (Fig. 4C) with exacerbation of liver injury (Fig. 4D), suggesting that
185 these T and B cells do not contribute to susceptibility to the LPS challenge.

186 Recent studies have demonstrated that NK cells are also IFN-γ–producing cells
187 that are recruited to the hepatic tissue during MAFLD and that they are also involved
188 in systemic inflammatory responses, including sepsis (24–29). We observed that NK
189 cell numbers were increased in the liver of PBS-treated MAFLD mice when compared
190 with mice fed a control diet (Fig. 4E). LPS challenge led to an increased accumulation
191 of NK1.1^{+}CD3^{-} NK cells in the liver of MAFLD mice, whereas NK1.1^{+}CD3^{+} NKT cells
192 were not detected (Fig. S3C and 4E). Furthermore, our cytometric analyses
193 demonstrated that NK cells infiltrated in the liver tissue secrete high levels of IFN-γ
194 (Fig.S3D and 4F). Next, to confirm the pathological involvement of NK cells during
195 hyperinflammation in MAFLD, we depleted these cells by treating animals with anti-
196 NK antibody 1.1, one day before the LPS challenge (Fig. S4). Interestingly, the
197 pharmacological depletion of NK cells in MAFLD animals provoked an increased
198 survival index (Fig. 4G). Furthermore, when NK cells were depleted, MAFLD animals
199 exhibited reduced hepatic damage (Fig. 4H), IFN-γ levels (Fig. 4I), and TNF-α levels
200 (Fig.4J). Together, these results suggest that NK cells are responsible for susceptibility
201 via IFN-γ production in MAFLD during endotoxemia.

202

203 **Neutrophils are responsible for susceptibility during hyperinflammation**
204 **in MAFLD**

205 During MAFLD development, innate immune cells, such as monocytes and
206 neutrophils, are the first leukocytes recruited to the liver (24, 30). With this in mind,
207 mice with MAFLD were challenged with LPS, and the infiltration of these cells in the

208 liver was quantified. During the initial inflammatory phase, six hours after the LPS
209 challenge, we observed that monocytes were recruited to the site (Fig. 5A and 5B).
210 Since inflammatory monocytes emigrate from the bone marrow towards the periphery
211 via CCR2 and then migrate to inflamed tissues, differentiating into monocyte-derived
212 macrophages (30, 31), we investigated the functional role of monocytes in MAFLD,
213 using CCR2-deficient mice (Fig. 5S). Interestingly, animals deficient in monocyte
214 migration (CCR2-/-) showed a high mortality rate compared to wild type after LPS
215 challenge and neutrophil migration was not altered (Fig. 5SA and Fig. 5SB). Moreover,
216 CCR2-/- animals subjected to the respective diets had leukocyte CD45+ infiltration
217 similar to that observed in the LPS challenge control mice (Fig. 5SC and Fig. 5SD).
218 Furthermore, the survival rate of MAFLD CCR2-/- mice challenged with LPS was not
219 different of MAFLD wild type mice also challenged with LPS (Fig. 5SB). Together, the
220 results suggest that monocytes do not contribute to susceptibility in endotoxemic
221 animals with MAFLD
222 In addition to monocytes, granulocytes are innate immune cells recruited to the
223 hepatic tissue during the development of MAFLD (19). We observed that high levels
224 of neutrophils are present in the hepatic tissue of animals with MAFLD and that their
225 recruitment is exacerbated in the hepatic microenvironment in endotoxemic mice (Fig.
226 5A and 5C). It is known that neutrophils are recruited to the inflammatory focus via
227 CXCR2 (32). To understand the involvement of these receptors and neutrophils in
228 MAFLD during endotoxemia, MAFLD animals were pre-treated one day before the
229 LPS challenge with CXCR2i or with anti-Ly6G, which depletes these cells throughout
230 the organism. Interestingly, after both treatments, we observed a reduction of the
231 leukocyte infiltration into the hepatic tissue (Fig. 5D) and a decrease in hepatic lesions
232 (ALT) (Fig. 5E) and TNF-α levels (Fig. 5F). Confirming the participation of granulocytes
233 in susceptibility after the LPS challenge in MAFLD, animals treated with CXCR2i and
234 anti-Ly6G showed an improvement in their survival (Fig. 5G and 5H).
235
236 **IFN-γ induces CD274 expression during endotoxemia in animals with**
237 **MAFLD**
238 IFN-γ is a cytokine that plays a crucial role in the T and NK cell-mediated
239 immune response (27–29, 33–35). Recent studies have shown that this inflammatory
240 cytokine also induces the expression of checkpoint molecules, such as programmed
241 death-ligand 1 (PD-L1), in different immune cells, including neutrophils (30, 36, 37).

242 Analyzing datasets from mice with MAFLD, we observed the upregulation of the
243 CD274 (PD-L1) gene and TNF-α in neutrophils and IFN-γ in NK cells (Fig. 1C, Fig1D,
244 and Fig. 1E). Considering these findings, we investigated whether IFN-γ induces the
245 expression of PD-L1 in neutrophils in MAFLD mice during endotoxemia. First, we
246 observed that only the MAFLD diet caused a significant increase in PD-L1 expression
247 in CD45+CD11b+ leukocytes after LPS challenge (Fig. S6C). Analysis of this
248 population revealed that neutrophils expressed higher levels of PD-L1 compared with
249 monocytes (Fig. 6SA–6SD). Moreover, PD-L1^{+} neutrophils exhibited increased
250 hepatic infiltration (Fig. 6A and 6B). Next, to confirm the role of IFN-γ in the expression
251 of PD-L1, we investigated whether IFN-γ is capable of increasing the expression of
252 PD-L1 in neutrophils after the LPS challenge of MAFLD. Mice with MAFLD lacking
253 IFN-γ were challenged with LPS and assessed for PD-L1 expression in granulocytes.
254 Interestingly, in the absence of IFN-γ, neutrophils do not express PD-L1, and their
255 infiltration in the liver was attenuated (Fig. 6C and 6D).
256 As demonstrated previously in sepsis, PD-L1 neutrophils showed reduced rates
257 of apoptosis (36). Therefore, we cultured neutrophils in the presence of IFN-γ and/or
258 LPS and assessed their apoptosis rate. Interestingly, in these *in vitro* conditions,
259 neutrophils expressing PD-L1 showed reduced rates of apoptosis (Fig. 6E and 6F),
260 suggesting that PD-L1-expressing neutrophils can survive for long periods in the
261 hepatic environment in MAFLD, accentuating the LPS-induced inflammatory
262 response.
263
264 **Neutrophils expressing PD-L1+ secrete TNF-α during hyperinflammation**
265 **in MAFLD**
266 There is also evidence that excessive secretion of TNF-α by immune cells,
267 especially neutrophils, may be associated with liver damage and the progression of
268 MAFLD (36, 37). To investigate a possible link between the expression of PD-L1 by
269 the neutrophils and their ability to express TNF-α, mice undergoing MAFLD were
270 exposed to LPS, and the expression of TNF-α by PD-L1+ neutrophils was assessed.
271 We observed an exacerbated expression of TNF-α by PD-L1+ neutrophils from
272 MAFLD when compared to control animals (Fig. 7A, Fig. 7B, Fig. 7D and Fig8SG) and
273 no increase in TNF-α^{+}PDL1^{-} neutrophils (Fig. 7C). These results illustrate that after
274 exposure of MAFLD animals to LPS, the expression of PD-L1 by neutrophils is linked
275 to heightened TNF-α expression compared to control animals fed standard chow. To

assess whether the lack of TNF-α signaling immunomodulates the granulocytic recruitment to the liver tissues in MAFLD animals, TNF receptor R1 and R2 knockout animals (TNF R1R2) were exposed to LPS. It was also observed that the absence of TNF-α did not interfere with the recruitment of neutrophils to the liver tissue (Fig. S8A and Fig. S8C) or the expression of PD-L1 in neutrophils (Fig. S8B and Fig. S8D). Similarly, the absence of TNF-α receptors in MAFLD during the challenge with LPS did not interfere with the production of IL-10 and IFN-γ (Fig. S8E and Fig. S8F). However, as described above, the absence of the TNF R1R2 receptor reduced liver injury and mortality induced by LPS administration in MAFLD (Fig. 3D and Fig. 3F).

Considering that NK cells present in liver tissue secrete IFN-γ (Fig. 4E) and that in IFN-$\gamma^{-/-}$ animals, there is a reduction in TNF-α levels in the liver of mice with MAFLD during endotoxemia (Fig. 4K), we next examined whether PD-L1+TNF-α+ neutrophils are present in MAFLD animals depleted of NK cells. It was observed that in the absence of NK cells, PD-L1+TNF-α+ neutrophils were not detected (Fig. 7E, Fig. 7F, and Fig. 7G), confirming that IFN-γ secreted by NK cells is crucial for inducing PD-L1 expression and TNF-α secretion by neutrophils in the hepatic tissue in MAFLD animals after LPS administration.

Anti-PD-L1 treatment protects animals with MAFLD during hyperinflammation

Next, we investigated the potential role of PD-L1 in TNF-α production by neutrophils and in the lesions in MAFLD mice. Initially, we found that anti-PD-L1, a biological drug inhibiting PD-L1's interaction with PD-1, effectively prevented liver inflammation and tissue damage (Fig. 8A, Fig. 8B, and Fig. 8F). Additionally, this treatment reduced liver TNF-α levels without affecting IFN-γ (Fig. 8C) and improved host survival (Fig. 8D). Importantly, anti-PD-L1 did not decrease the number of recruited NK cells in all groups studied (Fig. 8I and Fig. 8L). Notably, treatment with anti-PD-L1 successfully blocked LPS-induced neutrophil recruitment and the increased presence of PD-L1-expressing neutrophils in mice on HFCD (Fig. 8J and Fig. 8K), while these parameters remained unchanged in mice fed a standard chow diet (Fig8G, Fig8H). Overall, our findings suggest that anti-PD-L1 therapy primarily suppresses exaggerated TNF-α production by neutrophils in MAFLD mice without affecting the IFN-γ secretory activity of NK cells mechanistically.

310

311 ## 3. DISCUSSION

312 The pathogenesis of MAFLD and sepsis had been considered two independent
313 conditions, associated with local and systemic inflammatory response, respectively.
314 MAFLD is a chronic liver dysfunction characterized by the buildup of fat in the liver in
315 individuals who do not consume excessive amounts of alcohol. On the other hand,
316 sepsis is an inflammatory state triggered by an infection that leads to damage to vital
317 organs, including the lungs and liver. This occurs when the body's immune response
318 fails to contain the microorganisms at the site of the primary infection(9). Recent
319 studies demonstrate that the presence of MAFLD is associated with an increased risk
320 of developing sepsis (38, 39), but the exact mechanisms underlying this association
321 are not fully understood. In the present study, we observed that MAFLD mice induced
322 by an HFDC diet are more susceptible to a systemic and hepatic hyper-inflammatory
323 state induced by endotoxemia, confirming in our experimental condition that MAFLD
324 can be considered a crucial risk factor of sepsis progression, even when MAFLD or
325 hepatic inflammation is not yet detected. The LPS administration promotes the
326 polarization of a specific subset of granulocytes expressing PD-L1, which secrete high
327 levels of TNF-α in an NK-derived IFN-γ dependent manner. The released TNF-α plays
328 an important role in the liver lesion. We also observed that CD4+ and CD8+ T cells or
329 monocyte cells do not seem to participate in the mice's susceptibility in this hyper-
330 inflammatory state. In accordance, previous studies implicated NK cells in liver injuries
331 in different MAFLD and sepsis experimental models(25, 40–44). It was observed that
332 during severe sepsis, NK cell-released IFN-γ play a detrimental role in mediating
333 tissue injury (44). Similarly, in MAFLD, NK cells can accumulate in the liver and release
334 IFN-γ, which contributes to the development of hepatic inflammation and fibrosis(45).
335 Therefore, these studies, support that the increase in NK cells induced by
336 endotoxemia in MAFLD animals, along with IFN-γ secretion, appears to have a crucial
337 role in the increased susceptibility of these pathological conditions, contributing to
338 disease progression.

339 Considering this evidence, we re-analyzed previously published bioinformatic
340 data (21, 22) and observed that, in MAFLD patients, IFN-γ and TNF-α are up-
341 regulated, and that, in high-fat high fructose diet-fed mice, there is up-regulation of
342 IFN-γ in NK cells, and TNF-α and CD274 (PD-L1) in myeloid cells (21, 22), suggesting
343 that similar immune dysfunctions are observed in patients and experimental models

344 of MAFLD. To add experimental information about how the IFN-γ mediates the liver
345 lesion, we demonstrated that in endotoxemic MAFLD animals hepatic neutrophils are
346 important producers of TNF-α, and this release is stimulated by NK-derived IFN-γ
347 signaling. In addition, IFN-γ promoted the differentiation of PDL-1-expressing
348 neutrophils, given that in those animals depleted of NK, the neutrophils did not exhibit
349 this activated phenotype. Moreover, the PDL-1-expressing neutrophils showed a
350 reduced apoptosis rate, increasing the retention time of the neutrophils in hepatic
351 tissue. Thus, these events could explain the increase in hepatic injury in MAFLD
352 animals during endotoxemia. According, in the context of infection-triggered
353 inflammation, the participation of IFN-γ in modulating neutrophil pro-inflammatory
354 profiles, including the expression of PD-L1, has been demonstrated (36). Neutrophils,
355 as frontline innate immune cells, control pathogens through phagocytosis and the
356 release of microbial mediators, including cytokines, cytosolic enzymes, free radicals,
357 and NETs (46, 47). However, excessive neutrophil activity can lead to tissue damage,
358 particularly in sepsis, where they contribute significantly to multi-organ damage via the
359 overproduction of inflammatory mediators, including TNF-α (16, 48, 49). Our data
360 demonstrate that during MAFLD, liver neutrophils are major sources of TNF-α
361 production induced by endotoxemia. Confirming the involvement of TNF-α release by
362 PDL-1+ neutrophils stimulated by NK cells-derived IFN-γ in the increase of
363 susceptibility of MAFLD, we demonstrated that the absence of TNF-α signaling or
364 depleted NK cells led to improved survival in mice with MAFLD during endotoxemia.
365 However, the absence of TNF-α signaling did not affect PD-L1 expression in
366 neutrophils. These findings imply that, while TNF-α plays a crucial tissue lesions, its
367 intracellular signaling does not notably impair the expression of PD-L1 in the
368 neutrophils or their migration into liver tissue during MAFLD. To reinforce that
369 neutrophils are the main source of the TNF-α involved in susceptibility of MAFLD by
370 endotoxemia, we evaluate whether the neutralization of these cells with specific
371 antibodies could improve the survival of endotoxemic HFDC-fed mice. Numerous
372 strategies for targeting neutrophils are being investigated in various clinical and
373 experimental settings (12, 50), including the use of CXCR2 inhibitors in patients with
374 NASH (13, 50). Interestingly, we demonstrated that targeting neutrophils with different
375 biological drugs, similar to the inhibition of TNF-α, mitigated inflammation-induced liver
376 lesions.

377 Recent studies suggest that during the progression of MAFLD, PD-L1 is
378 expressed in both parenchymal and non-parenchymal cells (10, 51). Given that the
379 neutrophils responsible for hepatic damage in endotoxemic MAFLD mice exhibit a
380 specific PD-L1-expressing phenotype, *we* demonstrated that anti-PD-L1 significantly
381 reduced TNF-α-producing PD-L1+ neutrophils in the liver environment, attenuating
382 endotoxemia-induced inflammation and liver damage, ultimately reducing mortality in
383 MAFLD mice. This highlights the role of PD-L1 expression in neutrophils in promoting
384 a proinflammatory phenotype associated with heightened TNF-α production and
385 susceptibility of endotoxemic HFDC-fed mice. In the context of endotoxemia, recent
386 research indicates that PD-L1-expressing neutrophils also contribute to
387 immunosuppression and increased susceptibility to secondary infections (52) and also
388 contribute to lung injury. Thus, our data support that the inhibition of PD-L1, besides
389 preventing the organ lesions induced by sepsis in MAFLD patients, could also prevent
390 the long-term immunosuppression observed in these patients.

391 Although macrophages, including Kupffer cells, have been considered a
392 relevant source of cytokines in endotoxemic animals (53, 54), we did not find an
393 important role for these cells expressing CCR2 in the aggravation of endotoxemia,
394 since the absence of these chemokine receptor, which governs the migration and
395 differentiation of inflammatory monocytes into macrophages, did not influence the
396 endotoxemia mortality in animals with MAFLD. However, it's worth noting that we did
397 not extensively investigate the interaction of IFN-γ and TNF-α in the role of monocytes
398 in our model, necessitating further studies to unravel the possible mechanisms of
399 these cells.

400 Our study presents several limitations that should be acknowledged and
401 discussed. First, we cannot entirely rule out the possibility that our mice deficient in
402 pro-inflammatory components exhibit reduced responsiveness to LPS. However, our
403 ex vivo analyses using splenocytes from these animals revealed a preserved cytokine
404 production following LPS stimulation. These results suggest that the in vivo differences
405 observed are primarily driven by the MAFLD condition rather than by intrinsic defects
406 in LPS sensitivity. Second, the absence of publicly available single-cell RNA-seq
407 datasets from MAFLD subjects under endotoxemic or septic conditions limited our
408 ability to perform direct translational comparisons. To overcome this, we analyzed
409 existing MAFLD patients and experimental MAFLD datasets, which consistently
410 demonstrated upregulation of IFN-γ and TNF-α inflammatory pathways in MALFD. In

line with these findings, our murine model revealed TNF-α$^+$ myeloid and IFN-y$^+$ NK cell populations, thereby reinforcing the validity and translational relevance of our results.

Overall, our findings establish a biological basis for understanding the progression of endotoxemia in MAFLD, highlighting the dysregulated role of neutrophils in which hepatic metabolic syndrome potentiates the inflammatory effects of granulocytes via NK cells, advocating interventions to mitigate this inflammatory condition.

445

446 **4. MATERIAL AND METHODS**

447 **Experimental Design**

448 This study was designed to interrogate the pathologic mechanisms in MAFLD
449 during endotoxemia-induced generalized inflammation. The mice were submitted to
450 the HFDC diet for two weeks, and subsequently, LPS administration and the cellular
451 mechanisms were outlined after 6h of the challenge, knowing that no animal
452 succumbed to death (indicated by survival). Furthermore, knockout animals and those
453 treated with pharmacological inhibitors or neutralizing antibodies shared the same
454 control groups (chow and HFCD), as required by the animal ethics committee.
455 Inflammatory infiltrates along with liver lesions were assessed based on H&E-stained
456 tissue sections, and endpoint analyses included flow cytometry.

457

458 **Animals**

459 The mice used in this study were in the C57BL/6 genetic background and
460 included CCR2 $^{-/-}$, IFN-γ$^{-/-}$, and TNFR1R2 $^{-/-}$. Male mice aged 5 to 6 weeks were reared
461 and maintained under specific pathogen-free conditions in the University of São Paulo
462 vivarium, FMRP/USP. All animals received food and water ad libitum, at 25°C, with
463 food and water ad libitum. Mice were fed a standard low-fat diet (hereinafter referred
464 to as the standard "Chow" diet – 10% of calories derived from fat) or a Choline
465 Deficient High Fat Diet (referred to as "HFCD", 60% of calories derived from fat and
466 choline-deficient) for 2 weeks for the development of MAFLD. The diets were provided
467 by Rhoster (Araçoiaba da Serra- São Paulo). Care for the mice complied with
468 institutional guidelines on ethics in animal experiments; approved by CETEA (Ethics
469 Committee for Animal Experimentation of the Faculty of Medicine of Ribeirão Preto,
470 approved protocol number 193/2019).

471

472 **Endotoxemia**

473 Lipopolysaccharide (LPS; Escherichia coli (O111:B4), L2630, Sigma-Aldrich,
474 St. Louis, MO, USA) was administered intraperitoneally (i.p.; 10 mg/kg) in C57BL/6,
475 CCR2 -/-, IFN-γ-/-, and TNFR1R2 -/- mice. The HFCD was initiated in 5–6 week-old
476 mice, and LPS was administered after 2 weeks on the diet, meaning that LPS
477 administration occurred when the mice were 7–8 weeks old, with body weights ranging

478 from 22 to 26 g. LPS was previously solubilized in sterile saline and frozen at -70°C.
479 The animals were euthanized 6 hours after LPS administration.
480
481 **Survival analysis**
482 Survival was monitored daily, and survival curves were generated using the
483 Kaplan–Meier method. Experimental groups were composed of five animals per group
484 (n = 5), in accordance with the requirements of the institutional animal ethics
485 committee and the use of shared control groups. Sample size was defined based on
486 an a priori power analysis, which indicated that this number of animals per group was
487 sufficient to detect biologically relevant differences in survival with adequate statistical
488 power. Survival distributions among groups were compared using the log-rank
489 (Mantel–Cox) test. Statistical significance was considered when $p < 0.05$.
490
491
492 **Hepatic non-parenchymal cell isolation**
493 Livers were collected, and 200-300 mg of tissue was taken for flow cytometry
494 analysis. The tissue was minced with surgical scissors and then digested with 1 mg of
495 collagenase II, and 60 U/ml of DNase I in PBS at 37 °C for 45 minutes, shaking at 110
496 rpm. The digested tissue was then processed through a 100 µm cell strainer and
497 centrifuged at 1,500 rpm for 5 minutes. Subsequently, the isolation of non-
498 parenchymal cells was performed by Percoll (GE Healthcare) centrifuged at 2300rpm
499 at 22 °C for 30 minutes, subjected to ACK (red blood cell lysis), and resuspended in
500 0.5% BSA in PBS for staining. Single-cell suspensions were stained with Zombie Aqua
501 viability stain (Biolegend), blocked with TruStain FcX (Biolegend), and then stained
502 with flow cytometry antibodies when indicated; antibodies are tabulated in Table S1.
503 As animals were already in a hyperinflammatory state, no additional in vitro stimulation
504 was required. Intracellular detection of IFN-γ and TNF-α was conducted using the
505 Foxp3 staining kit (eBioscience). Since both antibodies were conjugated to PE,
506 staining and analyses were performed in separate experiments. Cells were collected
507 on the CANTO II flow cytometer using BD FACS Diva software and then analyzed
508 using FlowJo (USA).
509
510 **Histology**

511 Mouse livers were fixed in 10% formalin overnight, washed twice with PBS, and
512 placed in 70% ethanol or PBS until processing. For H&E, tissues were embedded in
513 paraffin, sectioned, and stained with H&E at the MGH Histopathology Research Core.
514
515 **Cytokine quantification**
516 For the detection of IFN-γ, TNF-α, and IL-10 in the liver, tissue samples were
517 weighed and titrated in 1 mL of PBS Complete (Roche Diagnostics, Mannheim,
518 Germany) containing a cocktail of protease inhibitors. Cytokine levels were determined
519 using commercial ELISA kits for IFN-γ, TNF-α, and IL-10 (Biolegend, USA).
520 Wavelength correction and background signals were subtracted from absorbance
521 values
522
523 **Serum analysis**
524 At the time of sacrifice, blood samples were collected in EDTA collection tubes
525 and subsequently centrifuged to obtain serum. Serum ALT and Urea levels were
526 measured using a colorimetric kit (BioQuant, Heidelberg, Germany) according to the
527 manufacturer's instructions.
528
529 **Neutrophil targeting**
530 For neutrophil targeting, antibodies/inhibitors were used as follows: Anti-Ly6G
531 (BioXCell, catalog # BP0075) was administered at 500 mg/kg per mouse on day 13
532 after starting the diet (24h before inoculation of the LPS) and sacrificed on day 14. For
533 survival studies, all mAbs were inoculated once daily for 7 days. CXCR2 inhibitor SB
534 225002 (Tocris, catalog #2725/10) was injected at 200 mg per dose and programmed
535 as anti-Ly6G. For anti–PD–L1–based neutrophil targeting, anti–PD-L1 (BioXCell,
536 catalog #BE0101) was injected at 12.5 mg/kg ~12h before the LPS challenge and
537 again 1 day after treatment, each time followed by anti-mouse IgG2b (12.5 mg/kg)
538 (BioXCell, catalog no. BE0252). All injections were intraperitoneal.
539
540 **Neutrophil purification and apoptosis assay**
541 Peripheral blood samples were collected by venipuncture and centrifuged at
542 450 × g for plasma separation. The blood cells were then resuspended in Hank's
543 balanced salt solution (Corning; cat. 21-022-CV), and the neutrophil population was
544 isolated by Percoll density gradient (GE Healthcare; cat. 17-5445-01) (72 %, 63%,

545 54% and 45%). Isolated neutrophils were resuspended in RPMI1640 (Corning; cat.
546 15-040-CVR) supplemented with 0.5% BSA. Neutrophil purity > 95% was determined
547 by Rosenfeld color Cytospin (Laborclin; cat 620529)
548 To quantify apoptosis, cells were permeabilized with Triton X-100 and stained
549 with propidium iodide. After 10 minutes of incubation at 4 degrees in the dark,
550 neutrophil apoptosis was quantified as PI+ staining on FACSCanto II (Becton
551 Dickinson, Franklin Lakes, NJ, USA). Results were analyzed using Flowjo software
552 (Tree Star, Ashland, OR, USA). Apoptosis was detected as a measure of the
553 hypodiploid peak in PI fluorescence histograms, as described by Nicoletti et al. BD
554 Bioscience, Franklin Lakes, NJ, USA) and Annexin V and 7-AAD double staining
555 (Biolegend, San Diego, USA).
556
557 **Splenocyte culture**
558 Mice were fed a control chow or HFCD diet for 2 weeks. Animals were
559 euthanized, and spleens were aseptically removed in cold PBS (Gibco) and then
560 mechanically dissociated through a 100-μm cell strainer to obtain a single-cell
561 suspension. Red blood cells are lysed with ACK buffer for 1–2 min at room
562 temperature, the reaction is quenched with complete RPMI 1640 medium
563 (supplemented with 10% heat-inactivated FBS, 2 mM L-glutamine, and antibiotics),
564 and cells are centrifuged and resuspended at the desired density, 1×10^6 cells/mL.
565 Splenocytes are plated in 96-well plates and incubated at 37°C, 5% CO_2. To induce
566 immune activation, cells are stimulated with lipopolysaccharide (E. coli O111:B4) at
567 concentrations ranging from 100 ng/mL to 1 μg/mL for 24 h, and cytokine dosage was
568 performed for IL-6 and TNF-α.
569
570 **NK cell depletion**
571 For in vivo NK cell depletion, male C57BL/6 mice received NK cell neutralizing
572 antibody (BioXCell, catalog # PK136) or isotype-matched mouse IgG2α monoclonal
573 antibody control (BioXCell, catalog # BE0252) by intraperitoneal injection (150 μg in
574 200 μL PBS 24h before LPS challenge). To assess survival, the antibodies were
575 inoculated 24 hours before the LPS challenge and then once a day for 7 days.
576
577 **Single-cell RNA sequencing analysis**

578 We re-analyzed single-cell transcriptomic data (GSE166504) from the mouse
579 liver from mice with MAFLD and their respective control groups (21). The dataset was
580 downloaded, and the RDS file was imported into R (55) environment version v4.2.3
581 and Seurat v4.1.1 (56) by filtering genes expressed in at least 300 cells. For the pre-
582 processing step, outlier cells were filtered out based on three metrics (library size <
583 20,000, number of expressed genes between 200 and 4,000, and mitochondrial
584 percentage expression < 0,8). The top 3,000 variable genes were then identified using
585 the 'best' method using the FindVariableFeatures function. Percent of mitochondrial
586 genes was regressed out in the scaling step, and Principal Component Analysis (PCA)
587 was performed using the top 3,000 variable genes, and the top 30 PCs were selected
588 for dimension reduction by Uniform Manifold Approximation and Projection (UMAP).
589 Clusters were identified using the author's annotation. Then, differential gene
590 expression analysis was performed using the FindAllMarkers function in Seurat with
591 default parameters to obtain a list of significant gene markers for each cluster of cells.
592 Visualization of genes illustrating expression levels was performed using R/Seurat
593 commands (DimPlot, FeaturePlot, and DotPlot) using ggplot2 (57) and customized
594 (58) R packages.
595
596 **RNA sequencing analysis**
597 RNA-seq data were obtained from GSE185051 (59). The R/Bioconductor
598 package edgeR was used to identify differentially expressed genes among the
599 samples, after removing absent features (zero counts in more than 75% of samples)
600 (60). Genes with a fold change of >0.5 were identified as differentially expressed.
601
602 **Pathway enrichment analysis**
603 The list of differentially expressed genes was enriched using the ClusterProfiler
604 R package (8). Gene ontology (GO) terms in the Biological Processes category with
605 P < 0.05 were considered significant. Statistically significant, non-redundant GO-
606 enriched terms were plotted.
607
608 **Statistics**
609 Statistical significance was determined by two-tailed paired or unpaired
610 Student's t-test or one-way ANOVA followed by Tukey's post hoc test. Absolute
611 numbers and percentages were compared using Fisher's exact test. Spearman rank

order correlation (r) was calculated to describe the correlations. $P<0.05$ was considered statistically significant. Statistical analyses and graphics were performed using the GraphPad Prism 8.4.2 software.

Author contributions: CCOB, AK, and FQC designed the study. CCOB, AK, PSAA and GCMC performed the mouse experiments. CCOB, AK, and FQC wrote the manuscript. GVLS performed the bioinformatic analysis. CCOB, AK, LOL, TMC, JCFAF, and FQC reviewed the manuscript.

Competing interests

The authors declare no competing interests.

Funding

Funding The research received funding from São Paulo Research Foundation (FAPESP, 2009/54014-7, 2011/19670, 2012/10438-0 and 2013/08216-2, Center for Research in Inflammatory Diseases), Coodernação de Aperfeiçoamento de Pessoal de Nivel Superior (CAPES) and Conselho Nacional de Desenvolvimento Científico e Tecnológico (CNPq)

Acknowledgements

We thank members of Group FQC for their advice and clinical assistance, and Marcella, Sergio R. Rosa, Katia Santos, Ieda Schivo for technical assistance.

References

1. Younossi ZM, et al. Global epidemiology of nonalcoholic fatty liver disease—Meta-analytic assessment of prevalence, incidence, and outcomes. *Hepatology*. 2016;64(1):73–84.

2. Younossi Z, et al. Global burden of MAFLD and NASH: trends, predictions, risk factors and prevention. *Nature Reviews Gastroenterology & Hepatology 2017 15:1*. 2017;15(1):11–20.

3. Paik JM, et al. Changes in the Global Burden of Chronic Liver Diseases From 2012 to 2017: The Growing Impact of MAFLD. *Hepatology*. 2020;72(5):1605–1616.

4. Estes C, et al. Modeling the epidemic of nonalcoholic fatty liver disease demonstrates an exponential increase in burden of disease. *Hepatology*. 2018;67(1):123–133.

648 5. Wong RJ, Cheung R, Ahmed A. Nonalcoholic Steatohepatitis Is the Most
649 Rapidly Growing Indication for Liver Transplantation in Patients With
650 Hepatocellular Carcinoma in the U.S. [published online ahead of print: 2014].
651 https://doi.org/10.1002/hep.26986.

652 6. Schuster S, et al. Triggering and resolution of inflammation in NASH
653 [preprint]. *Nat Rev Gastroenterol Hepatol*. 2018;15(6):349–364.

654 7. Peiseler M, Tacke F. Inflammatory Mechanisms Underlying Nonalcoholic
655 Steatohepatitis and the Transition to Hepatocellular Carcinoma. *Cancers*
656 *(Basel)*. 2021;13(4):1–26.

657 8. Carpino G, et al. Increased Liver Localization of Lipopolysaccharides in
658 Human and Experimental MAFLD. *Hepatology*. 2020;72(2):470–485.

659 9. Ferro D, et al. New Insights into the Pathogenesis of Non-Alcoholic Fatty
660 Liver Disease: Gut-Derived Lipopolysaccharides and Oxidative Stress.
661 [published online ahead of print: 2020]. https://doi.org/10.3390/nu12092762.

662 10. Lombardi R, et al. PD-1/PD-L1 Immuno-Mediated Therapy in MAFLD:
663 Advantages and Obstacles in the Treatment of Advanced Disease. *Int J Mol*
664 *Sci*. 2022;23(5). https://doi.org/10.3390/IJMS23052707.

665 11. Smith SR, et al. The cooperative effects of TNF-alpha and IFN-gamma are
666 determining factors in the ability of IL-10 to protect mice from lethal
667 endotoxemia. *J Leukoc Biol*. 1994;55(6):711–718.

668 12. Abe T, et al. Epidemiology of sepsis and septic shock in intensive care
669 units between sepsis-2 and sepsis-3 populations: sepsis prognostication in
670 intensive care unit and emergency room (SPICE-ICU). *J Intensive Care*.
671 2020;8(1):1–9.

672 13. Sakr Y, et al. Open Forum Infectious Diseases Open Forum Infectious
673 Diseases ® Sepsis in Intensive Care Unit Patients: Worldwide Data From the
674 Intensive Care over Nations Audit. https://doi.org/10.1093/ofid/ofy313.

675 14. Mcdonald B, Kubes P. Neutrophils and intravascular immunity in the liver
676 during infection and sterile inflammation. *Toxicol Pathol*. 2012;40(2):157–165.

677 15. Jenne CN, Kubes P. Immune surveillance by the liver. *Nat Immunol*.
678 2013;14(10):996–1006.

679 16. Michels EHA, et al. Association between age and the host response in
680 critically ill patients with sepsis. *Crit Care*. 2022;26(1).
681 https://doi.org/10.1186/S13054-022-04266-9/FIGURES/5.

682 17. Bouza C, López-Cuadrado T. Epidemiology and Trends of Sepsis in Young
683 Adults Aged 20-44 Years: A Nationwide Population-Based Study. *J Clin Med*.
684 2019;9(1). https://doi.org/10.3390/JCM9010077.

685 18. Knoop ST, et al. Epidemiology and impact on all-cause mortality of sepsis
686 in Norwegian hospitals: A national retrospective study. *PLoS One*.
687 2017;12(11). https://doi.org/10.1371/JOURNAL.PONE.0187990.

688 19. Ebrahimi F, et al. Risk of Severe Infection in Patients With Biopsy-proven
689 Nonalcoholic Fatty Liver Disease – A Population-based Cohort Study. *Clinical*
690 *Gastroenterology and Hepatology*. 2023;21(13):3346-3355.e19.

691 20. Raubenheimer PJ, Nyirenda MJ, Walker BR. A Choline-Deficient Diet
692 Exacerbates Fatty Liver but Attenuates Insulin Resistance and Glucose
693 Intolerance in Mice Fed a High-Fat Diet. *Diabetes*. 2006;55(7):2015–2020.

694 21. Yao K, et al. Transcriptomic profiling of a multiethnic pediatric MAFLD
695 cohort reveals genes and pathways associated with disease. *Hepatol*
696 *Commun*. 2022;6(7):1598–1610.

697 22. Su Q, et al. Single-cell RNA transcriptome landscape of hepatocytes and
698 non-parenchymal cells in healthy and MAFLD mouse liver. *iScience*.
699 2021;24(11). https://doi.org/10.1016/J.ISCI.2021.103233.

700 23. Burke JD, Young HA. IFN-γ: A cytokine at the right time, is in the right
701 place. *Semin Immunol*. 2019;43. https://doi.org/10.1016/J.SMIM.2019.05.002.

702 24. Amer J, et al. Insulin signaling as a potential natural killer cell checkpoint in
703 fatty liver disease. *Hepatol Commun*. 2018;2(3):285–298.

704 25. Martínez-Chantar ML, Delgado TC, Beraza N. Revisiting the Role of
705 Natural Killer Cells in Non-Alcoholic Fatty Liver Disease. *Front Immunol*.
706 2021;12:640869.

707 26. Wang F, et al. Activated Natural Killer Cell Promotes Nonalcoholic
708 Steatohepatitis Through Mediating JAK/STAT Pathway. *Cell Mol Gastroenterol*
709 *Hepatol*. 2022;13(1):257.

710 27. He H, et al. NK cells promote neutrophil recruitment in the brain during
711 sepsis-induced neuroinflammation. *Sci Rep*. 2016;6.
712 https://doi.org/10.1038/SREP27711.

713 28. Jensen IJ, et al. Polymicrobial sepsis influences NK-cell-mediated
714 immunity by diminishing NK-cell-intrinsic receptor-mediated effector responses
715 to viral ligands or infections. *PLoS Pathog*. 2018;14(10).
716 https://doi.org/10.1371/JOURNAL.PPAT.1007405.

717 29. Kumar V. Natural killer cells in sepsis: Underprivileged innate immune
718 cells. *Eur J Cell Biol*. 2019;98(2–4):81–93.

719 30. Nati M, Chung K-J, Chavakis T. The Role of Innate Immune Cells in
720 Nonalcoholic Fatty Liver Disease Introduction: MAFLD and NASH. [published
721 online ahead of print: 2021]. https://doi.org/10.1159/000518407.

722 31. Li M, et al. Recent advances targeting C-C chemokine receptor type 2 for
723 liver diseases in monocyte/macrophage. *Liver Int*. 2020;40(12):2928–2936.

724 32. Metzemaekers M, Gouwy M, Proost P. Neutrophil chemoattractant
725 receptors in health and disease: double-edged swords. *Cellular & Molecular*
726 *Immunology 2020 17:5*. 2020;17(5):433–450.

727 33. Eriguchi Y, et al. Essential role of IFN-γ in T cell–associated intestinal
728 inflammation. *JCI Insight*. 2018;3(18).
729 https://doi.org/10.1172/JCI.INSIGHT.121886.

730 34. Lin Q, et al. IFN-γ-dependent NK cell activation is essential to metastasis
731 suppression by engineered Salmonella. *Nat Commun*. 2021;12(1).
732 https://doi.org/10.1038/S41467-021-22755-3.

733 35. Arase H, Arase N, Saito T. Interferon gamma production by natural killer
734 (NK) cells and NK1.1+ T cells upon NKR-P1 cross-linking. *J Exp Med*.
735 1996;183(5):2391–2396.

736 36. Wang J feng, et al. Upregulated PD-L1 delays human neutrophil apoptosis
737 and promotes lung injury in an experimental mouse model of sepsis. *Blood*.
738 2021;138(9):806–810.

739 37. Falcinelli M, et al. Propranolol reduces IFN-γ driven PD-L1
740 immunosuppression and improves anti-tumour immunity in ovarian cancer.
741 *Brain Behav Immun*. 2023;110:1–12.

742 38. Acharya C, Bajaj JS. Gut Microbiota and Complications of Liver Disease.
743 *Gastroenterol Clin North Am*. 2017;46(1):155–169.

744 39. Mohammad S, Thiemermann C. Role of Metabolic Endotoxemia in
745 Systemic Inflammation and Potential Interventions. *Front Immunol*. 2021;11.
746 https://doi.org/10.3389/FIMMU.2020.594150.

747 40. Chen Y, Tian Z. Roles of Hepatic Innate and Innate-Like Lymphocytes in
748 Nonalcoholic Steatohepatitis. *Front Immunol*. 2020;11.
749 https://doi.org/10.3389/FIMMU.2020.01500.

750 41. Hwang S, et al. Role of Neutrophils in the Pathogenesis of Nonalcoholic
751 Steatohepatitis. *Front Endocrinol (Lausanne)*. 2021;12.
752 https://doi.org/10.3389/FENDO.2021.751802.

753 42. Stiglund N, et al. Retained NK Cell Phenotype and Functionality in Non-
754 alcoholic Fatty Liver Disease. *Front Immunol*. 2019;10(JUN).
755 https://doi.org/10.3389/FIMMU.2019.01255.

756 43. Mantovani A, et al. Neutrophils in the activation and regulation of innate
757 and adaptive immunity. [published online ahead of print: 2011].
758 https://doi.org/10.1038/nri3024.

759 44. Zeerleder S, et al. Activated cytotoxic T cells and NK cells in severe sepsis
760 and septic shock and their role in multiple organ dysfunction. *Clin Immunol*.
761 2005;116(2):158–165.

762 45. Luo XY, et al. IFN-γ deficiency attenuates hepatic inflammation and fibrosis
763 in a steatohepatitis model induced by a methionine- and choline-deficient high-
764 fat diet. *Am J Physiol Gastrointest Liver Physiol*. 2013;305(12).
765 https://doi.org/10.1152/AJPGI.00193.2013.

766 46. Rosales C. Neutrophil: A Cell with Many Roles in Inflammation or Several
767 Cell Types? *Front Physiol*. 2018;9(FEB).
768 https://doi.org/10.3389/FPHYS.2018.00113.

769 47. Kanashiro A, et al. The role of neutrophils in neuro-immune modulation
770 HHS Public Access. https://doi.org/10.1016/j.phrs.2019.104580.

771 48. Tracey KJ, et al. Shock and tissue injury induced by recombinant human
772 cachectin. *Science*. 1986;234(4775):470–474.

773 49. Bordon J, et al. Understanding the roles of cytokines and neutrophil activity
774 and neutrophil apoptosis in the protective versus deleterious inflammatory
775 response in pneumonia. *Int J Infect Dis*. 2013;17(2).
776 https://doi.org/10.1016/J.IJID.2012.06.006.

777 50. Leslie J, et al. CXCR2 inhibition enables NASH-HCC immunotherapy. *Gut*.
778 2022;71(10):2093–2106.

779 51. Dong G, et al. Increased PD-L1 Restricts Liver Injury in Nonalcoholic Fatty
780 Liver Disease. *Oxid Med Cell Longev*. 2022;2022.
781 https://doi.org/10.1155/2022/5954437.

782 52. Thanabalasuriar A, et al. *H E A L T H A N D M E D I C I N E PD-L1 +*
783 *neutrophils contribute to injury-induced infection susceptibility*. 2021.

784 53. Huston JM, et al. Splenectomy inactivates the cholinergic antiinflammatory
785 pathway during lethal endotoxemia and polymicrobial sepsis. *J Exp Med*.
786 2006;203(7):1623–1629.

787 54. Fonseca MT, et al. A leukotriene-dependent spleen-liver axis drives TNF
788 production in systemic inflammation. *Sci Signal*. 2021;14(679).
789 https://doi.org/10.1126/SCISIGNAL.ABB0969.

790 55. R: a language and environment for statistical computing [Internet].
791 https://www.gbif.org/tool/81287/r-a-language-and-environment-for-statistical-
792 computing. Accessed April 18, 2024.

793 56. Hao Y, et al. Integrated analysis of multimodal single-cell data. *Cell*.
794 2021;184(13):3573-3587.e29.

795 57. Wickham H. ggplot2. [published online ahead of print: 2016].
796 https://doi.org/10.1007/978-3-319-24277-4.

797 58. scCustomize-package: scCustomize: Custom Visualizations & Functions
798 for... in samuel-marsh/scCustomize: Custom Visualizations & Functions for
799 Streamlined Analyses of Single Cell Sequencing [Internet].

https://rdrr.io/github/samuel-marsh/scCustomize/man/scCustomize-package.html. Accessed April 18, 2024.

59. Chen Y, Lun ATL, Smyth GK. From reads to genes to pathways: Differential expression analysis of RNA-Seq experiments using Rsubread and the edgeR quasi-likelihood pipeline. *F1000Res*. 2016;5. https://doi.org/10.12688/F1000RESEARCH.8987.2/DOI.

60. Wu T, et al. clusterProfiler 4.0: A universal enrichment tool for interpreting omics data. *Innovation (Cambridge (Mass))*. 2021;2(3). https://doi.org/10.1016/J.XINN.2021.100141.

Figure 1. Mice fed with a high-fat and choline-deficient (HFCD) diet develop Metabolic Dysfunction–Associated Steatotic Liver Disease (MAFLD) and are more susceptible to endotoxemia. (A) Schematic illustration of the experimental design. (B) Survival curves of mice with MAFLD (n=5) and Chow diet (controls) (n=5) which were injected intraperitoneally with LPS (10mg/kg) and the survival rates were determined daily for 7 days (C and D) Serum ALT and Urea levels from mice with MAFLD and Chow, 6 hours after LPS (10 mg/kg) and PBS administration (n=5). (E) Effect of LPS inoculation on histopathology (H&E stain) of liver from mice with MAFLD or controls (Chow diet). The results are expressed as the mean ± standard deviation (SD) from one representative experiment. Statistical analysis was performed using one-way ANOVA followed by Tukey's multiple comparison test. Statistical significance was determined with the following p-values: *$p < 0.05$, **$p < 0.01$, ***$p < 0.001$. Each experiment was independently repeated 2 times to ensure reproducibility of the findings.

Figure 2. The expression of genes from the inflammatory pathways of IFN-γ and TNF-α is increased during the development of MAFLD in mice and humans. (A) Volcano plots illustrating the fold change and P-value for gene expression comparisons between livers of MAFLD and healthy patients. Genes of interest are highlighted on the volcano charts. (B) Gene Ontology (GO) functional analysis of differentially expressed genes (DEGs). GO enrichment analysis of DEGs was conducted using DAVID, presenting the 20 most significantly ($P < 0.05$) enriched GO terms in biological process, molecular function, and cellular component categories. All

839 adjusted statistically significant values are presented as negative log-transformed
840 base 10 values. (C) UMAP plots depicting immune cells from the livers of mice
841 subjected to 30 weeks of HFCD diet compared to Chow diet. (D) Frequency
842 distribution of immune cell populations. (E) Expression levels of CD14, CD274, IFN-γ,
843 and TNF-α genes within hepatic immune cell populations.

844

845 **Figure 3. TNF-α and IFN-γ participate in susceptibility in mice with MAFLD to**
846 **endotoxemia.** (A) IFN-γ and (B) TNF-α secretion in the tissue livers of Chow and
847 MAFLD mice injected with LPS (10mg/kg) (n = 5). (C) Serum ALT levels from mice
848 with MAFLD and Chow and/or knockout of IFNγ (IFNγ-/-) and (D) TNF-α (TNFR1R2-
849 /-), 6 hours after 10 mg/kg LPS and PBS administration (n=5). (E) Effect of LPS
850 inoculation on liver histopathology from mice with MAFLD and Chow and/or knockout
851 of IFNγ-/- and TNF-α (TNFR1R2-/-). (F) Survival curves of mice with MAFLD (n=5)
852 and Chow (n=5) and/or knockout of TNF-α (TNFR1R2-/-) and (G) IFN-γ (IFN-γ-/-)
853 after intraperitoneal inoculation of LPS (10mg/kg). The results are expressed as the
854 mean ± standard deviation (SD) from one representative experiment. Statistical
855 analysis was performed using one-way ANOVA followed by Tukey's multiple
856 comparison test. Statistical significance was determined with the following p-values:
857 *p < 0.05, **p < 0.01, ***p < 0.001. Each experiment was independently repeated 2
858 times to ensure reproducibility of the findings.

859

860 **Figure 4. IFN-γ secreted by NK cells increases susceptibility of animals with**
861 **MAFLD to endotoxemia**. (A) CD4 IFN-γ^+ and (B) CD8 IFN-γ^+ T cell frequency in
862 animals with MAFLD and Chow 6h after LPS inoculation. (C) displays survival curves
863 of mice with MAFLD (n=5) and Chow (n=5) and T-cell knockout (RAg-/-). (D) Serum
864 ALT levels from mice with MAFLD in knockout of Rag -/-, 6 hours after 10 mg/kg LPS
865 (n=5). (E) and (F) represent the number of cells and frequency of NK IFNγ^+ or IFN-γ^-
866 in animals with MAFLD and Chow 6h after LPS inoculation (G) The survival curves of
867 mice with MAFLD (n=5) and Chow (n=5) and/or depleted NK cells (Anti NK 1.1), 6
868 days after intraperitoneal inoculation of LPS (10mg/kg) (H) presents the serum ALT
869 levels from mice with MAFLD and Chow of mice with MAFLD (n=5) and Chow (n=5)
870 and/or depleted NK cells (Anti NK 1.1), 6 hours after 10 mg/kg LPS or PBS
871 administration (n=5). (I) and (J) depict IFN-γ and TNF-α secretion in the livers of Chow
872 and MAFLD mice injected with LPS (10mg/kg) (n=5), respectively. (K) shows TNF-α
873 secretion in the livers of Chow and MAFLD and/or knockout of IFN-γ (IFNγ-/-) mice
874 injected with LPS (10mg/kg) (n=5)." The results are expressed as the mean ± standard
875 deviation (SD) from one representative experiment. Statistical analysis was performed
876 using one-way ANOVA followed by Tukey's multiple comparison test. Statistical
877 significance was determined with the following p-values: *p < 0.05, **p < 0.01, ***p <
878 0.001. Each experiment was independently repeated 2 times to ensure reproducibility
879 of the findings.

880

881

882

883

884

885 **Figure 5. Neutrophils but not monocytes mediate susceptibility of animals with**
886 **MAFLD to endotoxemia** (A) Representative flow cytometry plot showing monocytes
887 (CD45+CD11b+MHC-Ly6C+Ly6G-) and neutrophils (CD45+CD11b+MHC-
888 Ly6C+Ly6G+) and a number of monocytes (B) and neutrophils (C) in animals with
889 MAFLD and Chow after LPS inoculation. (D) Effect of LPS inoculation on liver
890 histopathology of mice with MAFLD and Chow treated with a CXCR2 inhibitor
891 (CXCR2i) and neutrophil-depleted animals (anti-Ly6G). (E) Serum ALT levels of mice
892 with MAFLD and Chow and/or CXCR2i and anti-Ly6G, 6 hours after administration of
893 10 mg/kg of LPS and PBS (n=5). (F) TNF-α secretion in the liver of Chow and MAFLD
894 mice injected with LPS (10mg/kg) (n = 5). (G) Survival curves of mice with MAFLD
895 (n=5) and Chow (n=5) treated with anti-Ly6G or (H) CXCR2i, and the survival rates
896 were analysed daily for 6 days after intraperitoneal administration of LPS (10mg/kg).
897 The results are expressed as the mean ± standard deviation (SD) from one
898 representative experiment. Statistical analysis was performed using one-way ANOVA
899 followed by Tukey's multiple comparison test. Statistical significance was determined
900 with the following p-values: *p < 0.05, **p < 0.01, ***p < 0.001. Each experiment was
901 independently repeated 2 times to ensure reproducibility of the findings.

902

903 **Figure 6. IFN-γ induces PD-L1 expression and reduces apoptosis in mouse**
904 **neutrophils with MAFLD.** (A) Representative flow cytometry plot showing the
905 expression of PD-L1 in gated neutrophils and (B) the quantification of PD-L1+
906 neutrophils in the liver of mice with MAFLD or that received Chow diet, 6 hours after
907 LPS inoculation (n=5 per group). (C) Representative flow cytometry plot showing the
908 expression of PD-L1 in gated neutrophils and (D) the quantification of PD-L1+
909 neutrophils in the liver of mice with MAFLD and Chow and/or IFNγ knockout (IFNγ-/-)
910 6 hours after LPS inoculation (n=5 per group). (E) Representative flow cytometry plot
911 showing the expression of PD-L1 and apoptosis (Annexin V+ 7AAD+) in gated
912 neutrophils and (F) the frequency of apoptosis in neutrophils cultured in medium, LPS,
913 IFN-γ, or LPS+ IFN-γ for 24 hours. The results are expressed as the mean ± standard
914 deviation (SD) from one representative experiment. Statistical analysis was performed
915 using one-way ANOVA followed by Tukey's multiple comparison test. Statistical
916 significance was determined with the following p-values: *p < 0.05, **p < 0.01, ***p <
917 0.001. Each experiment was independently repeated 2 times to ensure reproducibility
918 of the findings.

919

920

921 **Figure 7. IFN-γ-dependent secretion of TNF-α by PD-L1+ neutrophils induces**
922 **susceptibility of animals with MAFLD to endotoxemia**. (A) Representative flow
923 cytometry plot showing TNF-α expression in PD-L1+ neutrophils in the liver of animals
924 with MAFLD or fed with Chow diet 6h after LPS inoculation. (B) Number of TNF-α+
925 neutrophils. (C) Number of TNF-α+PD-L1- neutrophils. (D) number of TNF-α+PD-L1+
926 neutrophils. (E) Representative flow cytometry plot showing TNF-α expression in PD-
927 L1+TNF+ neutrophils in the liver of animals with MAFLD and Chow and/or depleted
928 NK cells (anti-NK 1.1) 6h after LPS inoculation. (F) Number of PD-L1+ neutrophils. (G)
929 Frequency of TNF-α+ neutrophils. The results are expressed as the mean ± standard
930 deviation (SD) from one representative experiment. Statistical analysis was performed
931 using one-way ANOVA followed by Tukey's multiple comparison test. Statistical
932 significance was determined with the following p-values: *$p < 0.05$, **$p < 0.01$, ***$p <$
933 0.001. Each experiment was independently repeated 2 times to ensure reproducibility
934 of the findings.

935

936 **Figure 8. Anti PD-L1 treatment reduces PD-L1 neutrophils in animals with**
937 **MAFLD during endotoxemia**. (A) Schematic illustration of experimental design. (B)
938 Serum ALT levels of mice with MAFLD or feded with Chow and/or treated with anti-
939 PDL1, 6 hours after administration of 10 mg/kg of LPS or PBS (n=5). (C) IFN-γ and
940 TNF-α secretion in the liver of Chow and MAFLD mice injected with LPS (10mg/kg)
941 treated with anti-PDL1 (n = 5). (D) Survival curves of mice with MAFLD (n=5) and
942 Chow (n=5) treated or not with anti-PD-L1. (E) Representative flow cytometry graph
943 showing TNF-α expression in PD-L1+ neutrophils in the liver of animals with MAFLD
944 and Chow and/or treated with anti-PD-L1 6h after LPS inoculation. (F) Effect of LPS
945 inoculation in liver histopathology of mice with MAFLD and Chow treated or not with
946 anti-PD-L1. (G and J) Frequency of PDL1 neutrophils, (H and K) Number of
947 neutrophils, (I and L) Number of NK cells from animals with MAFLD and Chow and/or
948 treated with anti-PDL1 after 6h of LPS inoculation. The results are expressed as the
949 mean ± standard deviation (SD) from one representative experiment. Statistical
950 analysis was performed using one-way ANOVA followed by Tukey's multiple
951 comparison test. Statistical significance was determined with the following p-values:
952 *$p < 0.05$, **$p < 0.01$, ***$p < 0.001$. Each experiment was independently repeated 2
953 times to ensure reproducibility of the findings.

954 **Figure S1. Validation of the HFCD-induced MAFLD experimental model based**
955 **on liver weight, blood glucose levels, and histological analysis (H&E and Picro**
956 **Sirius staining).**
957 (A) Liver height, (B) plasma glucose, and (C) representative liver histological sections
958 of lipid accumulation, steatotic morphology and collagen deposition (Picro Sirius Red
959 staining) of mice fed a high-fat, choline-deficient (HFCD) or control chow diet for two
960 weeks and subsequently challenged or not with LPS (10 mg/kg, i.p.)(n=5) (Data are
961 expressed as the mean ± standard deviation (SD) from one representative experiment.
962 Statistical analysis was performed using one-way ANOVA followed by Tukey's multiple

963 comparison test. Statistical significance was determined as *p < 0.05, **p < 0.01, ***p
964 < 0.001. Each experiment was independently repeated at least twice to ensure
965 reproducibility of the findings

966 **Figure S2. The IFNγ-deficient mice display LPS responses comparable to**
967 **controls.**
968 (A–B) Splenocytes isolated from C57BL/6 and IFNγ^{-}/$^{-}$ mice fed with Chow or HFCD
969 for two weeks were stimulated in vitro with LPS (100 ng/mL) for 24 hours. Cytokine
970 levels of (A) IL-6 and (B) TNF-α were quantified in the culture supernatants. Data are
971 expressed as mean ± standard deviation (SD) from one representative experiment (n
972 = 5 per group). Statistical analysis was performed using one-way ANOVA followed by
973 Tukey's multiple comparison test. Statistical significance was defined as *p < 0.05, **p
974 < 0.01, ***p < 0.001. Each experiment was independently repeated twice to ensure
975 reproducibility.

976 **Figure S3. NK cells produce high levels of IFN-γ during endotoxemia in MAFLD**
977 (A) Representative flow cytometry dot plot showing CD4^{+}IFN-γ^{+} T cells from the liver
978 of mice fed a high-fat, choline-deficient (HFCD) or chow diet for two weeks and
979 subsequently challenged or not with LPS. (B) Representative dot plot of hepatic
980 CD8^{+}IFN-γ^{+} T cells under the same experimental conditions. (C) Representative dot
981 plot showing NK cells (NK1.1^{+}CD3^{-}) from the liver of HFCD and chow-fed mice
982 challenged or not with LPS. (D) Representative dot plot of IFN-γ expression by NK
983 cells (NK1.1^{+}CD3^{-}) from the same groups.

984 **Figure S4. Anti-NK1.1 treatment depletes NK cells in animals with MAFLD during**
985 **endotoxemia**
986 (A) Representative flow cytometry dot plot showing depletion of NK cells
987 (NK1.1^{+}CD3^{-}) in the liver of mice fed a high-fat, choline-deficient (HFCD) or chow diet
988 for two weeks and challenged with LPS, following treatment with anti-NK1.1 antibody.

989 **Figure S5. Monocytes do not participate in the susceptibility of mice with**
990 **MAFLD to endotoxemia**
991 (A) Representative flow cytometry dot plot showing neutrophils (CD45^{+}CD11b^{+}Ly6G^{+})
992 and monocytes (CD45^{+}CD11b^{+}Ly6G^{-}) in the liver of C57BL/6 and CCR2^{-}/$^{-}$ mice fed
993 a high-fat, choline-deficient (HFCD) or chow diet for two weeks and challenged with
994 LPS. (B) Survival curves of C57BL/6 and CCR2^{-}/$^{-}$ mice under the same experimental
995 conditions. (C) Representative dot plot of total leukocytes (CD45^{+}) in the liver of
996 C57BL/6 and CCR2^{-}/$^{-}$ mice after LPS challenge. (D) Frequency of leukocytes (CD45^{+})
997 in the liver of C57BL/6 and CCR2^{-}/$^{-}$ mice fed HFCD or chow diet and challenged with
998 LPS (n=5). Data are representative of one experiment reproduced independently twice
999 with similar results. Statistical analysis was performed using one-way ANOVA followed
1000 by Tukey's multiple comparison test. Statistical significance was determined with the
1001 following p-values: *p < 0.05, **p < 0.01, ***p < 0.001. Results are expressed as the
1002 mean ± standard deviation (SD).

1003 **Figure S6. Neutrophils are the main PD-L1–expressing subset among**
1004 **CD45^{+}CD11b^{+} leukocytes in MAFLD.**(A and B) Representative flow cytometry
1005 histogram showing PD-L1 expression on neutrophils (CD45^{+}CD11b^{+}Ly6C^{+}Ly6G^{+}) and

monocytes ($CD45^+CD11b^+Ly6C^+Ly6G^-$) isolated from the liver of mice fed a high-fat, choline-deficient (HFCD) or control chow diet for two weeks and challenged with LPS (10 mg/kg, i.p.) (n=5) (C) Representative dot plot showing PD-L1 expression within total hepatic $CD45^+CD11b^+$ leukocytes from chow- and HFCD-fed animals for two weeks, either challenged or not with LPS. (D) Representative dot plot depicting the relative proportions of neutrophils($CD45^+CD11b^+Ly6C^+Ly6G^+$) and monocytes ($CD45^+CD11b^+Ly6C^+Ly6G^-$) within total $CD45^+CD11b^+$ leukocytes in the liver of chow- and HFCD-fed mice after LPS challenge (n=5). Data are expressed as the mean ± standard deviation (SD) from one representative experiment. Statistical analysis was performed using one-way ANOVA followed by Tukey's multiple comparison test. Statistical significance was determined as *$p < 0.05$, **$p < 0.01$, ***$p < 0.001$. Each experiment was independently repeated at least twice to ensure reproducibility of the findings.

Figure S7. CXCR2i treatment reduces IFN-γ in the liver tissue of animals with MAFLD during endotoxemia
(A) IFN-γ levels in the liver of mice fed a high-fat, choline-deficient (HFCD) or chow diet for two weeks, challenged with LPS, and treated with either anti-Ly6G antibody or a CXCR2 inhibitor (CXCR2i) (n=5).. (B) IL-10 levels in the liver of the same experimental groups (n=5). The data are representative of one experiment reproduced independently twice with similar results. Statistical analysis was performed using one-way ANOVA followed by Tukey's multiple comparison test. Statistical significance was determined with the following p-values: *$p < 0.05$, **$p < 0.01$, ***$p < 0.001$. Results are expressed as the mean ± standard deviation (SD).

Figure S8. TNFR1/R2^{-}/$^{-}$ animals do not show reduced neutrophil infiltration in the hepatic tissue of mice with MAFLD during endotoxemia. (A) Representative flow cytometry dot plot showing neutrophils ($CD45^+CD11b^+Ly6G^+$) in the liver of TNFR1R2$^+$/$^+$ and TNFR1R2$^-$/$^-$ mice fed a high-fat, choline-deficient (HFCD) or chow diet for two weeks and challenged with LPS. (B) Representative dot plot of PD-L1$^+$ neutrophils ($CD45^+CD11b^+Ly6G^+PD\text{-}L1^+$) under the same experimental conditions. (C) Quantification of neutrophils ($CD45^+CD11b^+Ly6G^+$) in the liver of TNFR1R2$^+$/$^+$ and TNFR1R2$^-$/$^-$ mice after LPS challenge. (D) Quantification of PD-L1$^+$ neutrophils ($CD45^+CD11b^+Ly6G^+PD\text{-}L1^+$) in the liver(n=5). (E) IL-10 levels in the liver of TNFR1R2$^+$/$^+$ and TNFR1R2$^-$/$^-$ mice fed HFCD or chow and challenged with LPS(n=5). (F) IFN-γ levels in the liver of TNFR1R2$^+$/$^+$ and TNFR1R2$^-$/$^-$ mice under the same conditions. (G) Representative histogram showing TNF-α expression in the liver of C57BL/6 mice fed HFCD or chow for two weeks, challenged or not with LPS. The data are representative of one experiment reproduced independently twice with similar results. Statistical analysis was performed using one-way ANOVA followed by Tukey's multiple comparison test. Statistical significance was determined with the following p-values: *$p < 0.05$, **$p < 0.01$, ***$p < 0.001$. Results are expressed as the mean ± standard deviation (SD).

1049

Figure 2. The expression of genes from the inflammatory pathways IFNγ and TNFα is increased during the development of MAFLD in mice and human

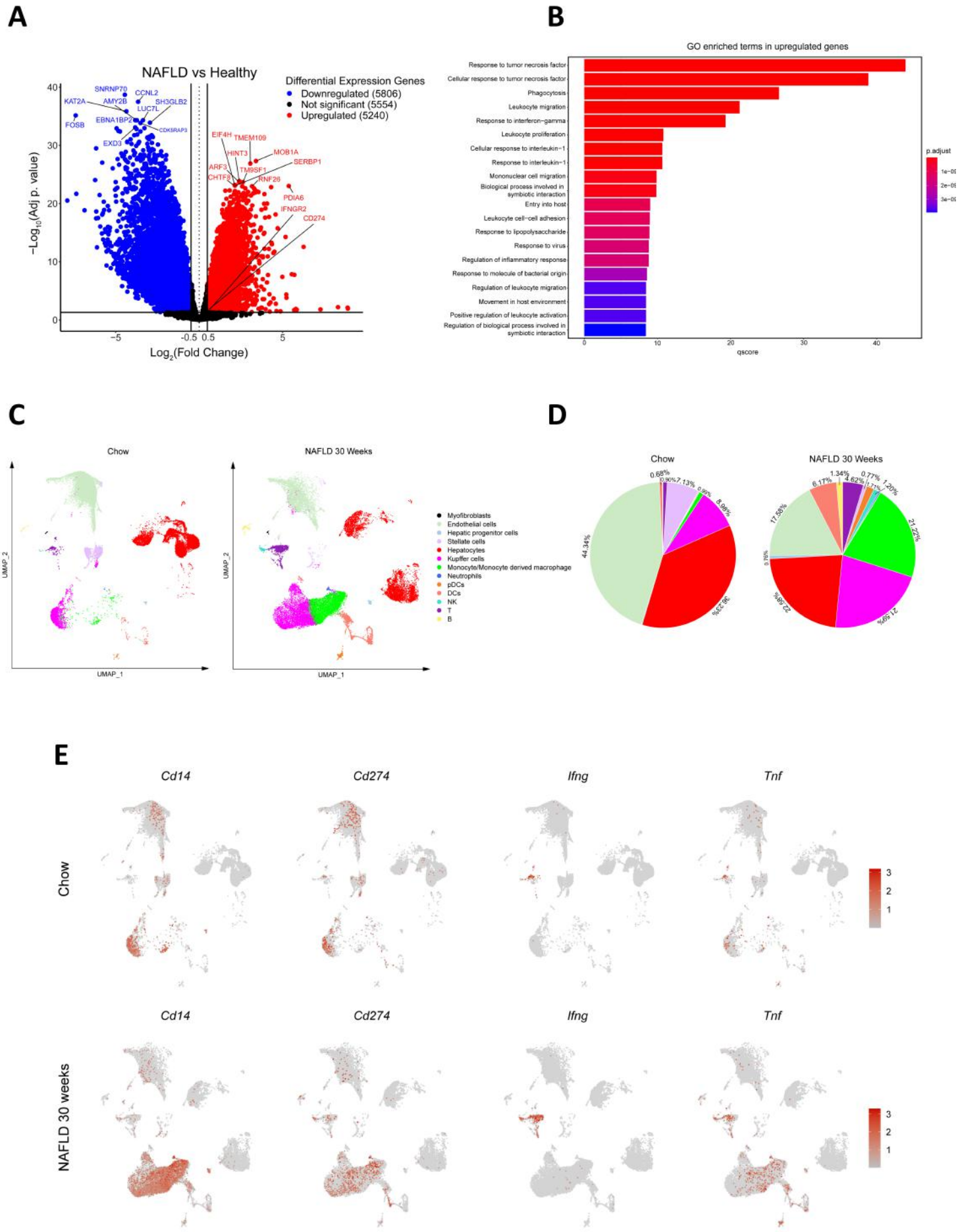

Figure 3. TNF-α and IFN-γ participate in susceptibility in mice with MAFLD to endotoxemia

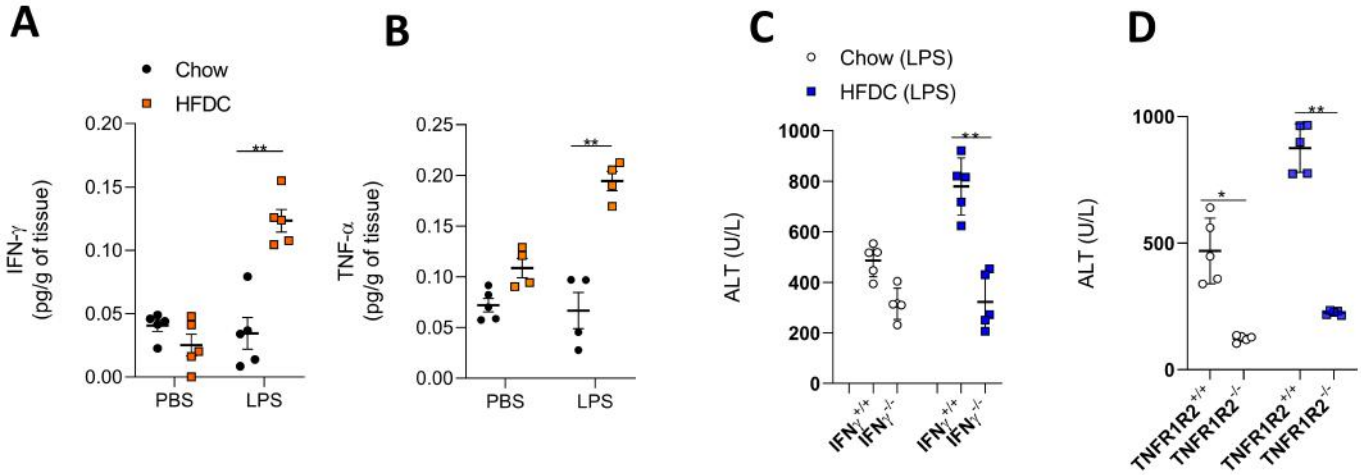

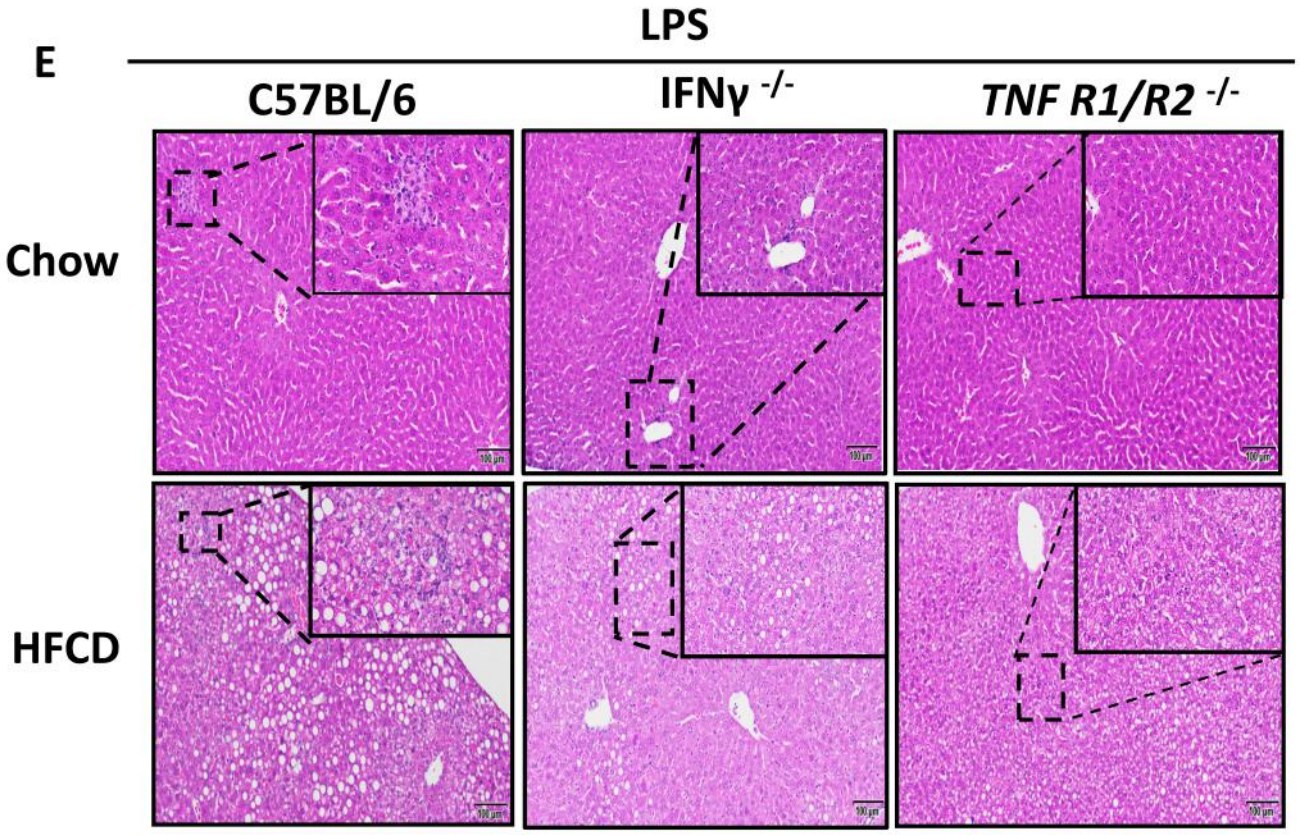

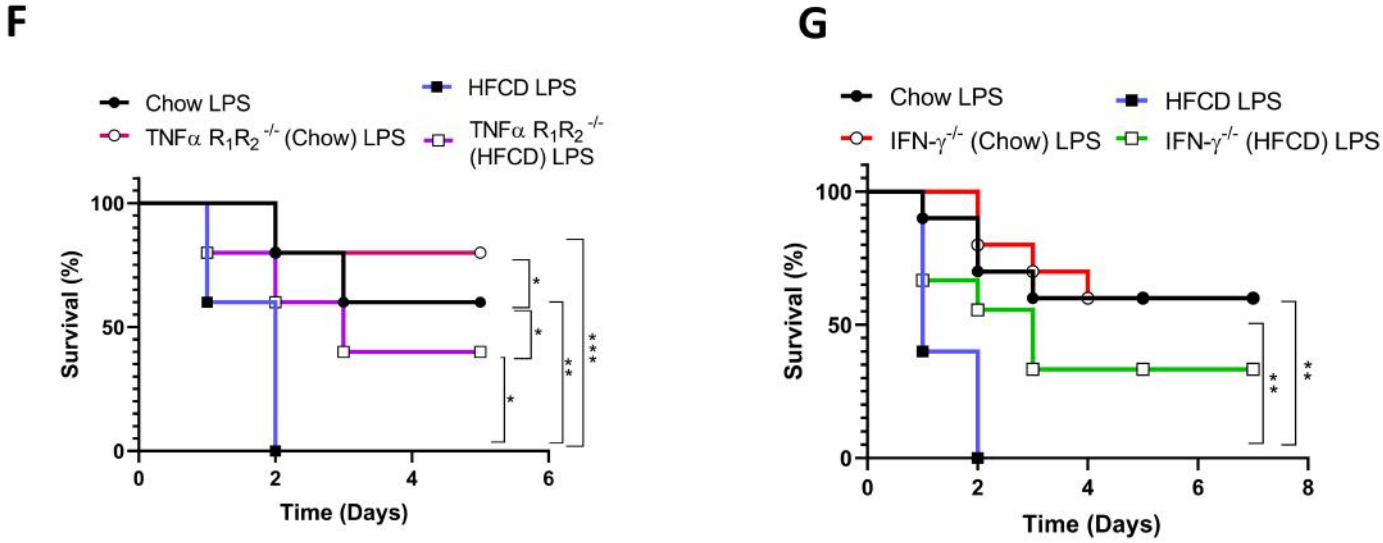

Figure 4. IFN-γ secreted by NK cells increases susceptibility of animals with MAFLD to endotoxemia

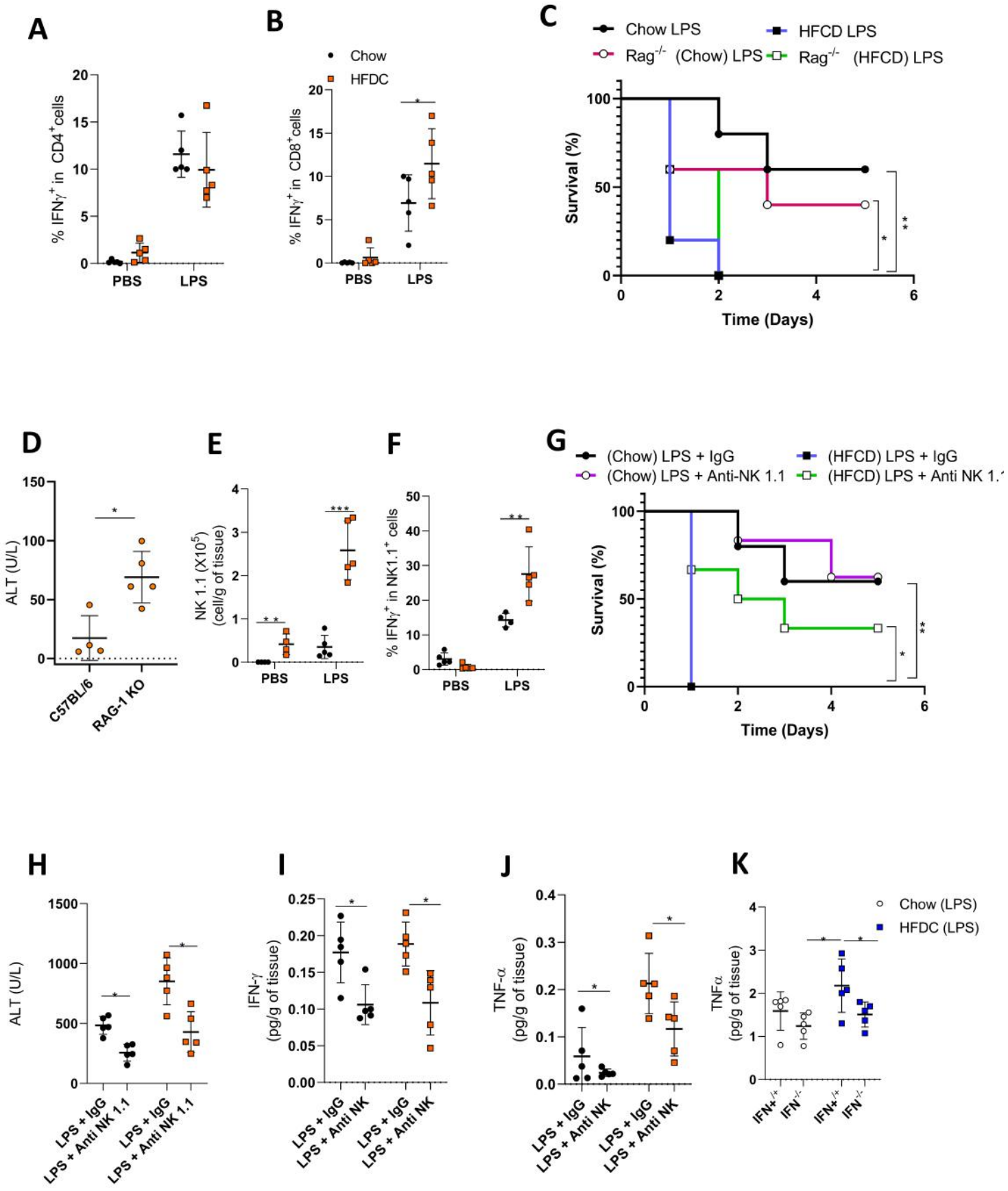

Figure 5. Neutrophils but not monocytes mediate susceptibility of animals with MAFLD to endotoxemia

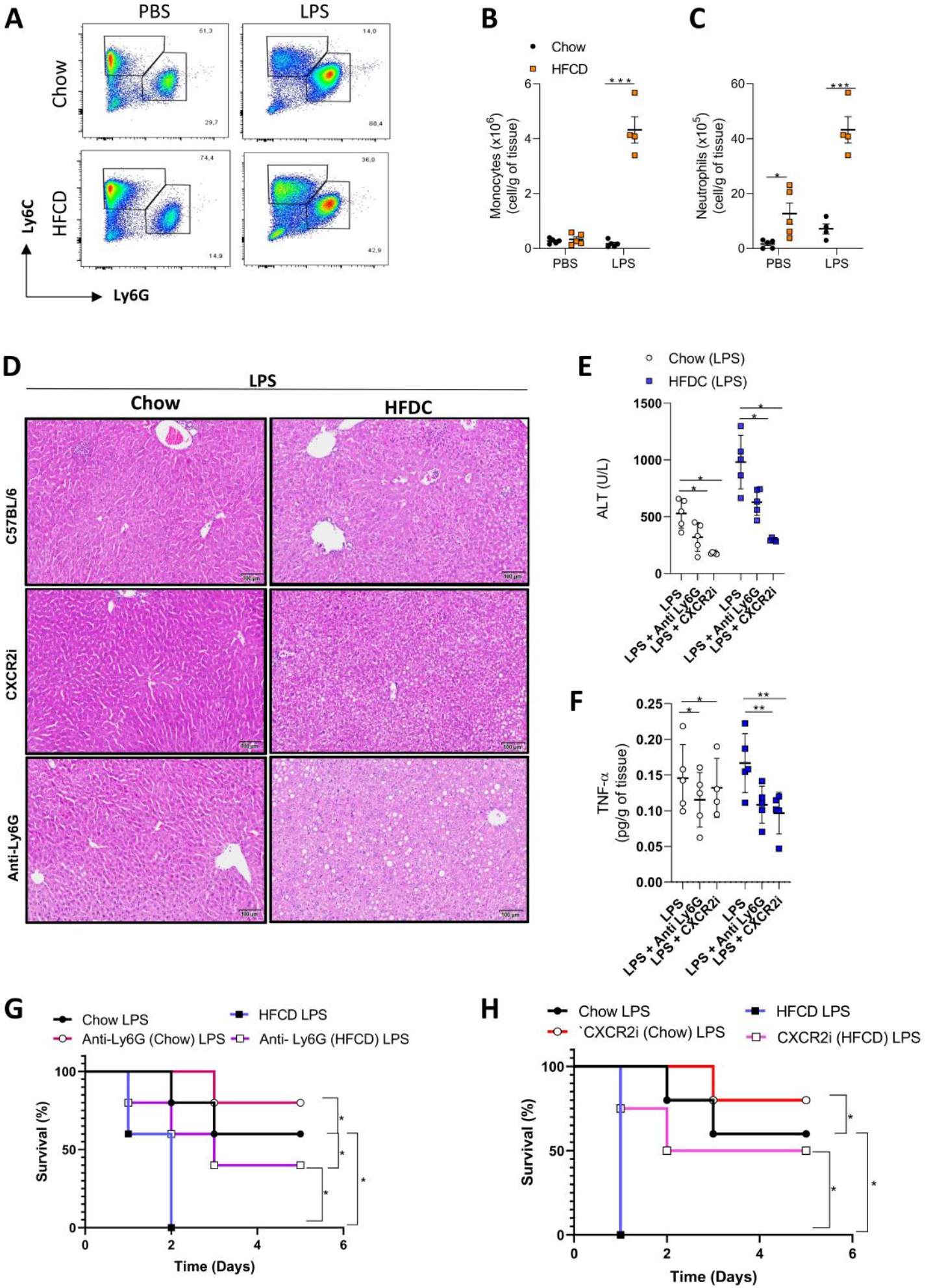

Figure 6. IFN-γ induces PD-L1 expression and reduces apoptosis in mouse neutrophils with MAFLD

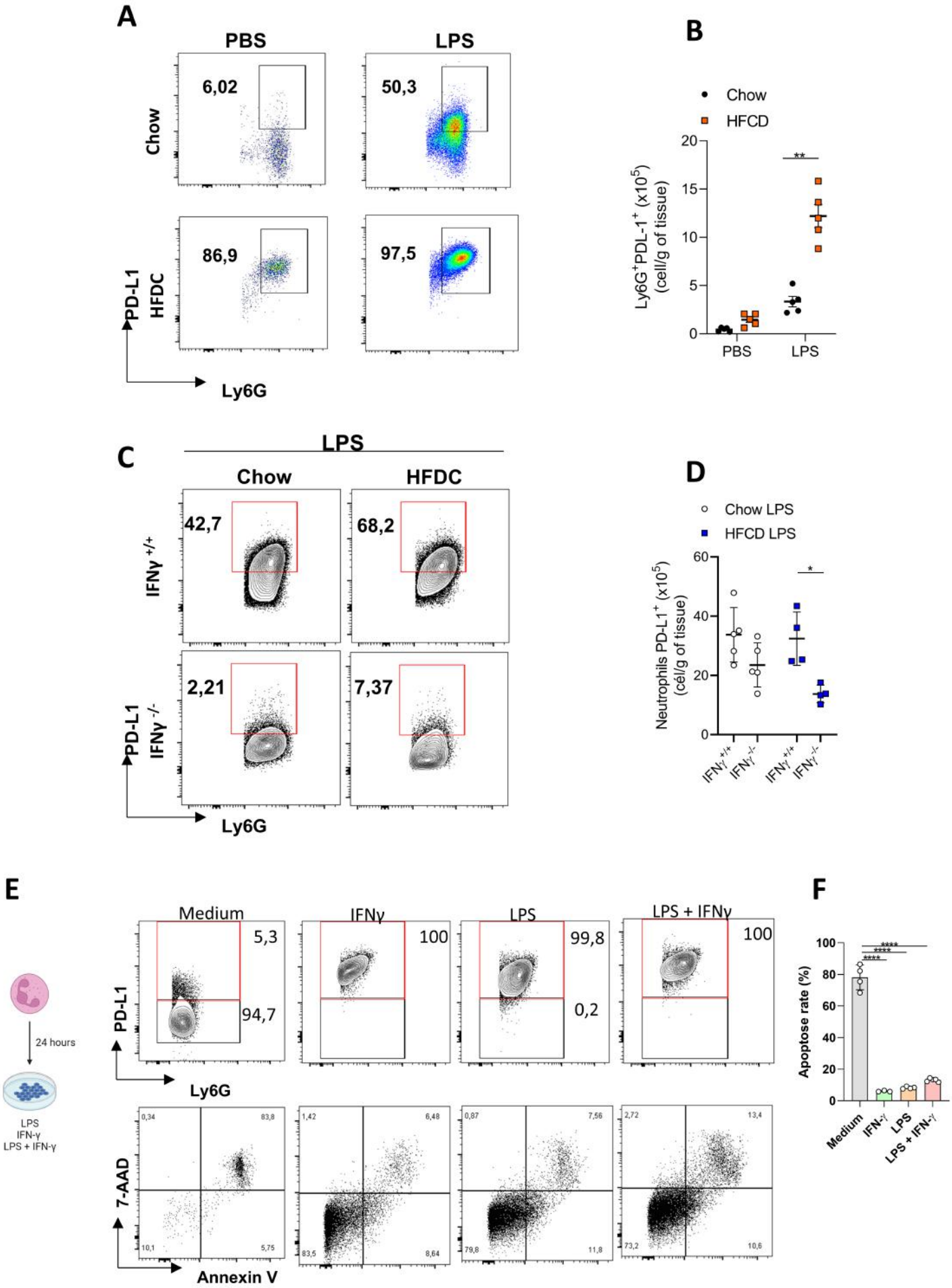

Figure 7. IFN-γ-dependent secretion of TNF-α by PD-L1+ neutrophils induces susceptibility of animals with MAFLD to endotoxemia

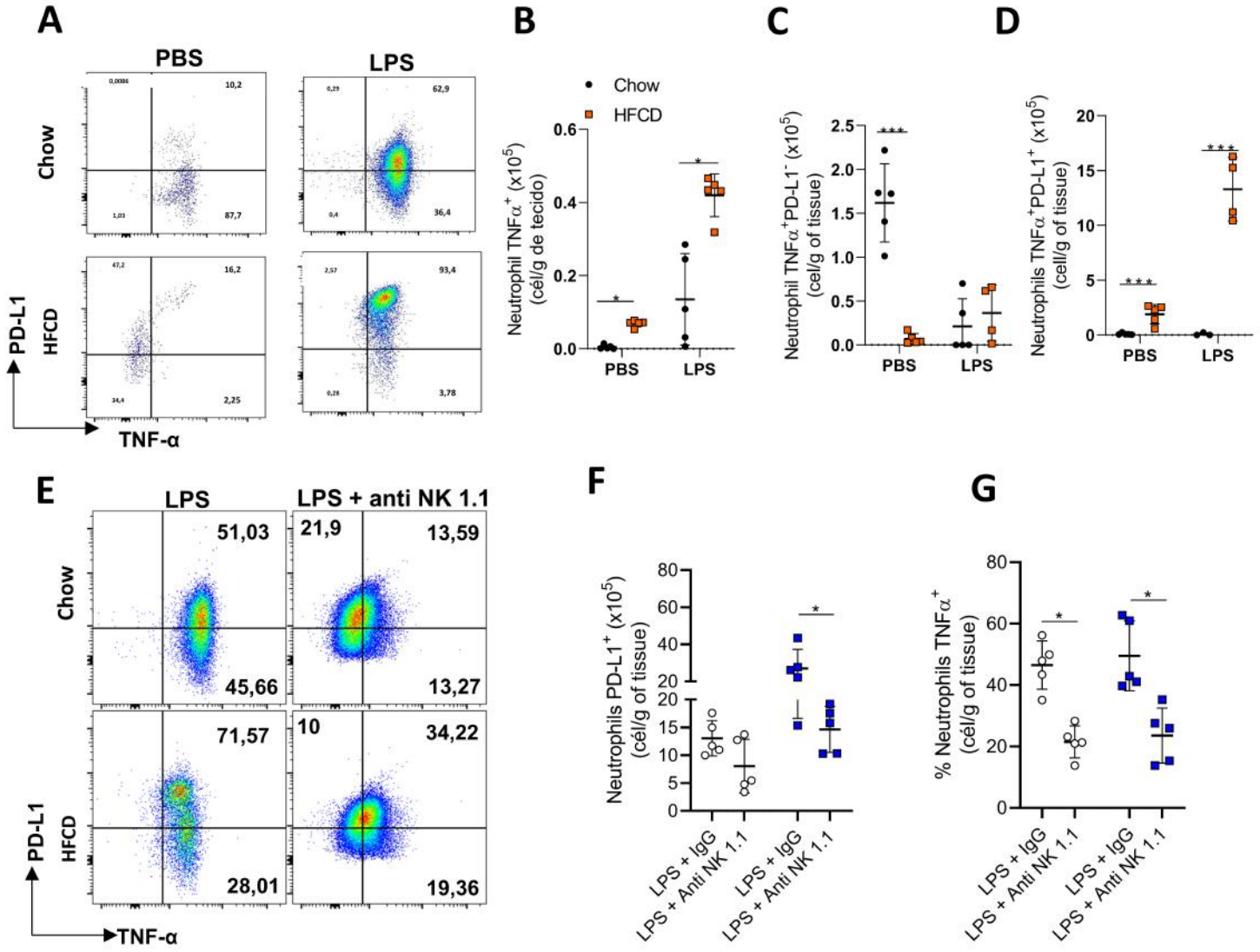

Figure 8. Anti PD-L1 treatment reduces PD-L1 neutrophils in animals with MAFLD during endotoxemia

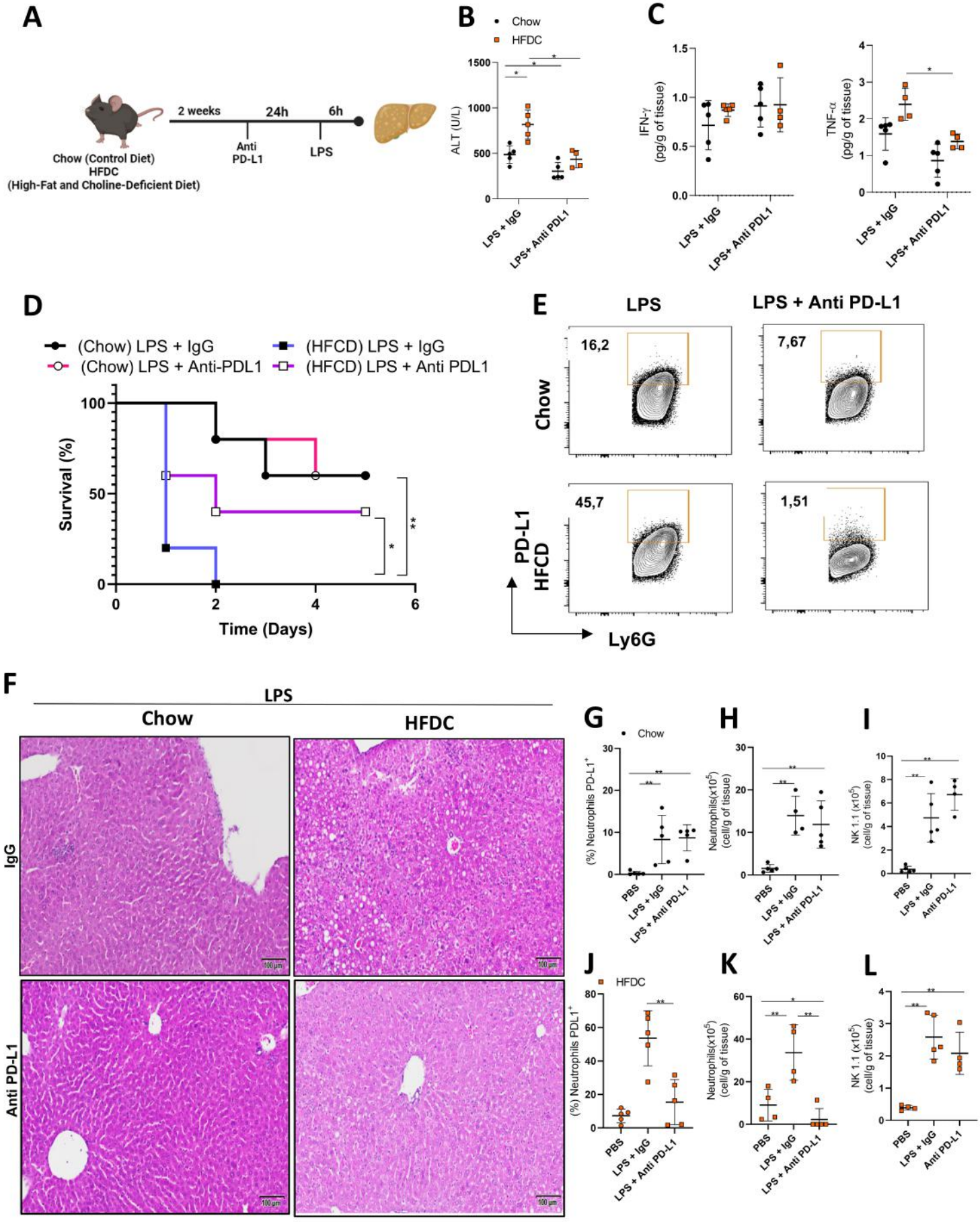
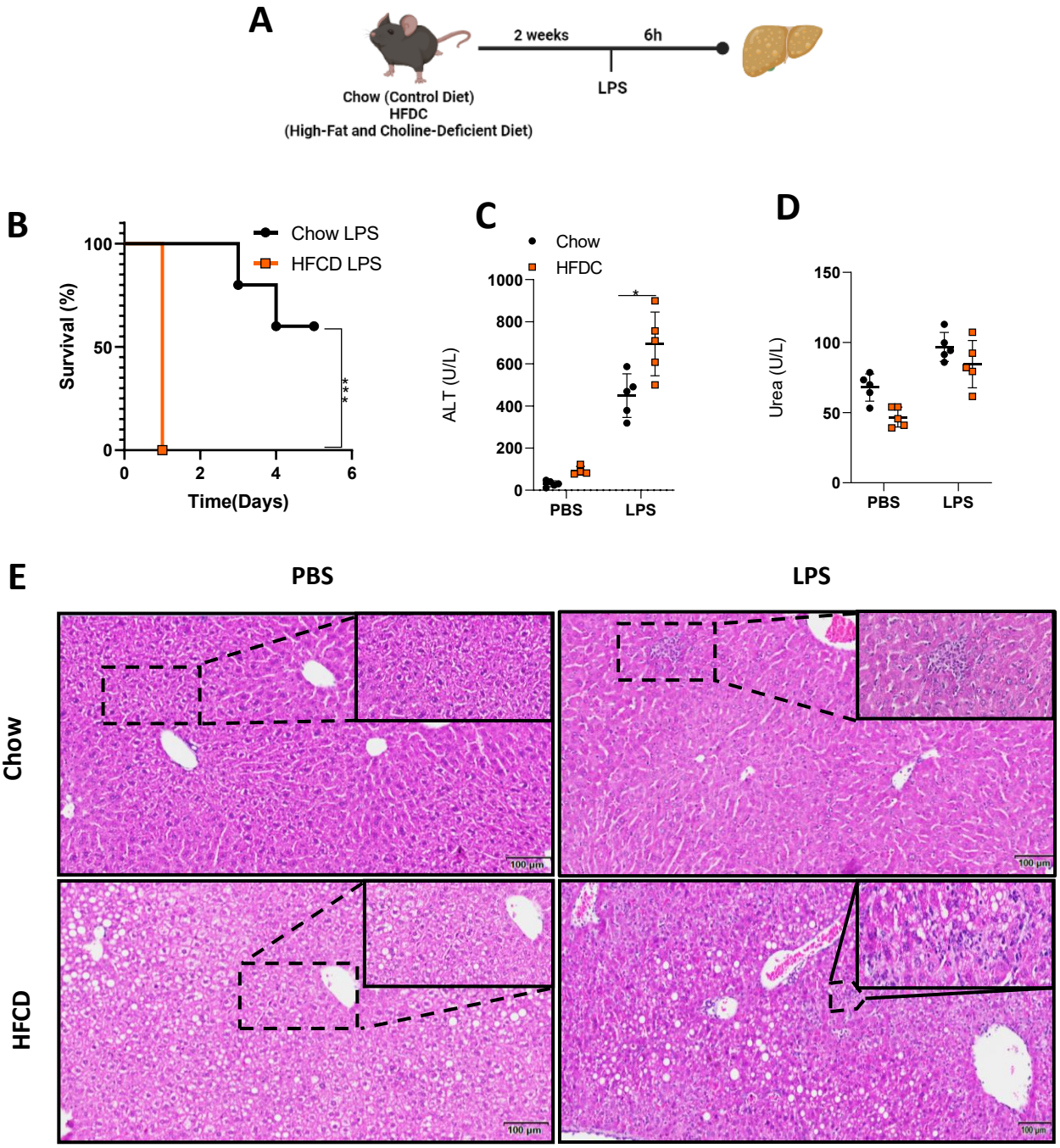
Figure 1. Mice fed with a high-fat and choline-deficient (HFCD) diet develop Metabolic Dysfunction–Associated Steatotic Liver Disease (MAFLD) and are more susceptible to endotoxemia